AD-A274 151

TNO-report

FEL-92-B438

copy nr.

/

title

**Over-the-horizon propagation measurements at six radar-frequency bands at the Atlantic Ocean coast**

author(s):

R.B. Boekema

DTIC
ELECTE
DEC 27 1993
S A

date:

July 1993

classification

| | |
|---|---|
| classified by | : H.J.M. Heemskerk |
| classification date | : juli 1993 |

TDCK RAPPORTENCENTRALE
Frederikkazerne, gebouw 140
v/d Burchlaan 31  MPC 16A
TEL. : 070-3166394/6395
FAX. : (31) 070-3166202
Postbus 90701
2509 LS Den Haag

| | |
|---|---|
| title | : ongerubriceerd |
| abstract | : ongerubriceerd |
| executive summary | : ongerubriceerd |
| report text | : ongerubriceerd |
| appendix A | : ongerubriceerd |

| | | |
|---|---|---|
| no. of copies | : 28 | |
| no. of pages | : 68 | (including Executive Summary and appendix, excluding RDP and distribution list) |
| no of appendices | : 1 | |

93-31052

**93 12 22 165**

# DISCLAIMER NOTICE

THIS DOCUMENT IS BEST QUALITY AVAILABLE. THE COPY FURNISHED TO DTIC CONTAINED A SIGNIFICANT NUMBER OF PAGES WHICH DO NOT REPRODUCE LEGIBLY.

I'T( · · ''Y INSPECTED 5

| | | |
|---|---|---|
| report no. | : | FEL-92-B438 |
| title | : | Over-the-horizon propagation measurements at six radar-frequency bands at the Atlantic Ocean coast |
| author(s) | : | R.B. Boekema |
| institute | : | TNO Physics and Electronics Laboratory |
| date | : | July 1993 |
| NDRO no. | : | |
| no. in pow '93 | : | 710.3 |
| Research supervised by | : | H.J.M. Heemskerk |
| Research carried out by | : | R.B. Boekema |

ABSTRACT (ONGERUBRICEERD)

In the autumn of 1989 the propagation subgroup of NATO AC/243 (Panel3/RSG8) has conducted a propagation experiment near Lorient France, at the Atlantic Ocean. Purpose of this experiment was to gain an insight into the influence of the evaporation duct above the sea on the propagation of radar signals of different frequencies in an over-the-horizon situation, and into the applicability of model predictions. Participating nations were the United States, France, Germany and the Netherlands. As Dutch representative, the TNO Physics and Electronics Laboratory has measured path losses continuously during a period of 52 days at 3, 5.6, 10.5, 16, 35 and 94 GHz for a 27.7 km over-the-horizon path. The geometry of the experiment has been chosen to represent a typical ship defence situation.

The measurements have shown that for the present case the nearly always present evaporation duct results in a signal enhancement with the strongest effects at the 10.5 and 16 GHz frequencies. An extended study of the quality of the model predictions, possible by the unique set of measurement results, shows some interesting matters. If we divide the process of prediction into two parts, the calculation of the duct height from the meteorological data and the path loss calculation from this duct height, we come to the conclusion that the first part is responsible for the largest inaccuracies. The used duct height calculation method showed systematic deviations for different meteorological conditions. The inaccuracy of the duct height calculation makes useful path loss predictions at the millimetre-wave frequencies (35 and 94 GHz) impossible for this over-the-horizon situation. The predictions at the lower frequencies are much better, but not always satisfactory. The deviation analyses in this report can be useful to improve propagation models.

| rapport no. | : | FEL-92-B438 |
| titel | : | Over-de-horizon propagatiemetingen op zes radarfrequentiebanden aan de Atlantische-Oceaankust |
| auteur(s) | : | Ing. R.B. Boekema |
| Instituut | : | Fysisch en Elektronisch Laboratorium TNO |
| datum | : | juli 1993 |
| hdo-opdr.no. | : | |
| no. In Iwp '93 | : | 710.3 |
| Onderzoek uitgevoerd o.l.v. | : | Ir. H.J.M. Heemskerk |
| Onderzoek uitgevoerd door | : | Ing. R.B. Boekema |

## SAMENVATTING (ONGERUBRICEERD)

In het najaar van 1989 heeft de propagatiesubgroep van NATO AC/243 (Panel3/RSG8) aan de Atlantische oceaankust bij het Franse Lorient een propagatie-experiment uitgevoerd. Het doel van dit experiment was inzicht te verkrijgen in de invloed van evaporation duct boven zee op de propagatie van radarsignalen van verschillende frequenties voor een over-de-horizon situatie, en in de bruikbaarheid van model voorspellingen. Deelnemende landen waren de Verenigde Staten, Frankrijk, Duitsland en Nederland. Het Fysisch en Elektronisch Laboratorium TNO heeft als Nederlandse vertegenwoordiger zorggedragen voor de padverliesmetingen van zes signalen met de frequenties 3; 5,6; 10,5; 16; 35 en 94 GHz die gedurende 52 dagen onafgebroken plaatsvonden over een 27,7 km lang traject. De gekozen geometrie van het experiment is representatief voor een typische scheepsverdedigingssituatie. De metingen tonen aan dat voor deze situatie de bijna constant aanwezige evaporation duct resulteert in een signaalverbetering, die zich het sterkst laat gelden bij 10,5 en 16 GHz. Uit een uitgebreid onderzoek naar de kwaliteit van de modelvoorspellingen, dat mogelijk was door de unieke set meetgegevens, zijn een aantal zaken naar voren gekomen. Als we de totstandkoming van een voorspelling splitsen in twee delen, de berekening van de ducthoogte uit de meteorologische waarnemingen en het berekenen van de padverliezen uit deze ducthoogten, dan blijkt het eerste deel verantwoordelijk te zijn voor de grootste onnauwkeurigheden. Voor de gebruikte ducthoogte-berekeningsmethode zijn systematische afwijkingen voor verschillende meteorologische situaties aan te geven. Voor de gemeten over-de-horizon situatie is de berekende ducthoogte onvoldoende nauwkeurig om zinvolle padverliesvoorspellingen te doen voor de millimetergolffrequenties (35 en 94 GHz). De voorspellingen voor de lagere frequenties zijn veel beter, maar blijken ook niet altijd bevredigend te zijn. De in dit rapport beschreven analyse van oorzaken kan bruikbaar zijn voor het verbeteren van propagatiemodellen.

# CONTENTS

# EXECUTIVE SUMMARY OF THE OVER-THE-HORIZON PROPAGATION MEASUREMENTS AT SIX RADAR-FREQUENCY BANDS AT THE ATLANTIC OCEAN COAST

## I.      BACKGROUND AND PURPOSE OF THE EXPERIMENT

In former experiments of the propagation subgroup of NATO AC/243 (Panel3/RSG8), which is responsible for millimetre wave studies, the influence of atmospheric refraction above the sea surface on the signal propagation was observed. The availability of new propagation models possible by increased computer performance and the conviction that the influence of propagation effects is large while the models need to be validated, were the motives for the subgroup to set up an extensive study of this subject. Two measurement campaigns were initiated in order to collect over-the-horizon propagation data in the most important radar frequency bands under various climatological circumstances. The analysis of the data gathered during the first experiment under moderate climate conditions is described in this report. This experiment was carried out in 1989 on the French Atlantic Ocean coast close to the town Lorient. The second experiment was performed under subtropical conditions at the French Mediterranean Sea coast in the summer of 1990, and is described in a separate report (FEL-93-A149). A comparison between the results of the two experiments is described in an other report (FEL-93-A150).

The experiments were focussed on the influence of evaporation ducting in a just over-the-horizon situation. The evaporation duct is a trapping layer caused by the characteristic refractivity profile in the lower atmosphere above sea due to the evaporation of the sea water. It extends from the sea surface to a few tens of meters above the water. It results in a refraction of electromagnetic waves above the surface and influences the propagation all along the path. The just over-the-horizon situation is of specific interest for the defence of warships. Firstly because the important first detection takes place at this distance, and secondly because the effects at this distance can be very large. A timely first detection of an attacking sea skimming missile is essential to the ship to organize its defence in time.

The experiment and analysis of the data reported here is set out to:

-    get a deeper understanding into the influence of evaporation
     ducting on the propagation of radar waves at different radar
     frequencies;

-    validate propagation models for short-term predictions;

-    point-out critical phases of the modelling process;

-    study the relation between the climate and ducting;

-    point-out properties of other types of ducting.

## II.        DESCRIPTION OF THE EXPERIMENT

Although also other propagation equipment was brought into action, this report is based only on the Dutch equipment.

Specific properties of the Lorient experiment are:

-        Atlantic ocean conditions;

-        Measurement period from September to November 1989;

-        52 days continuously monitored propagation and meteorological data;

-        Propagation data at 3, 5.6, 10.5, 16, 35, and 94 GHz, measured every 10 seconds;

-        Meteorological data measured every 10 seconds by a buoy halfway the propagation path;

-        27.7 km propagation path between the peninsulas Gâvres and Quiberon;

-        Transmitter heights of 8.5 m and receiver heights of 10.5 m above average sea level, with a maximum variation of 5 meter due to the tide;

-        Rough sea circumstances.

The one-way propagation measurements were performed by specially built equipment composed of CW transmitters and receivers with high gain antennas.

For the used geometry the propagation sets were situated at-the-horizon at very low ide situations and just over-the-horizon in all other cases.

Apart from the meteorological data from the buoy there was also some data support by coastal stations.

### III. PROPAGATION MODELLING

Propagation prediction is always executed in two stages. In the first stage the atmospheric refraction profile is obtained. The second stage of the prediction, the propagation model, determines the influence of the atmospheric refraction profile on the electromagnetic wave propagation.

For this experiment the first stage of modelling is performed by a duct height model called the Paulus model. This model calculates the duct height, as a measure of the atmospheric refraction profile, from four meteorological parameters. These are the air temperature, sea temperature, wind speed and humidity, all measured at sea, in this case by the buoy.

We can distinguish two meteorological conditions important for the calculation of the duct height. Dependent on the air-sea temperature difference, the atmosphere is called stable or unstable. When the sea temperature is higher than the air temperature, the atmosphere is in a thermally unstable condition. An air temperature higher than the sea temperature creates a thermally stable atmosphere condition.

Both the propagation behaviour and the duct height model performance are different for the two stability conditions.

The propagation loss model responsible for the second stage of the modelling process is performed by the PC-PEM model. This model uses the parabolic equation method to make propagation loss predictions at the used frequencies based on the duct height.

Only these models are used for the predictions. It is not the intention of this report to study the minor differences between several duct or propagation models. The aim is to get insight into the general performance of the models.

Some of the data of the experiment is used for a comparative duct model study by the French participants which will be published.

We can say that the used models performed good in comparison with other models.

## IV.        ANALYSIS OF GATHERED DATA

- Meteorological circumstances.

The buoy data measured during the experiment showed a variation of the individual parameters necessary for the duct height calculation. The data set provides probably a good characterization of the moderate Atlantic Ocean climate. Only a short period with a lot of fog and high humidity was notable and shows an unexpected influence on the data statistics.

- Long-term statistics.

Statistics of the path losses are derived to show the influence of ducting on the propagation at the different frequencies during the experiment.

The item considered is the enhancement factor calculated by subtracting the diffraction loss (the predicted path loss if there is no duct) from the measured path loss.

This results in different statistics for every frequency.

They show that the signal levels at all frequencies are almost always enhanced, sometimes with considerable values.

Predominant enhancement factors at the six frequencies 3, 5.6, 10.5, 16, 35 and 94 GHz are 6, 12, 18, 18, 12 and 6 dB.

More than 50% of the time the enhancement factors are higher than 5, 9, 15, 15, 11, 6 dB. This indicates that the 10.5 and 16 GHz frequencies are more enhanced than the higher and lower frequencies.

- Short-term comparison of measured and predicted path loss.

In an operational radar situation it is important to have an accurate short term propagation prediction. For every 10 minutes of the 52 days period of the campaign, the propagation predictions were calculated using the described models. These were compared directly with the measurements and presented graphically. The correlation between the measurements and predictions were in general not very satisfactory with average deviations round six dB. At the millimetre wave frequencies (35 and 94 GHz) the predictions were even very poor taking the smaller overall signal variation in account.

- Study of the prediction performance.

By analyzing the measurement data at the lowest frequencies and the propagation model it was

possible to relate the comparison between measurements and predictions to a comparison of duct heights.

This revealed that the deviation in the predictions was mainly caused by the duct height model. It also showed a large difference between the predictions calculated for a stable and an unstable atmosphere.

- Specific observations.

When the first stage of the modelling process is skipped and the path losses at different frequencies are computed for a given duct height, there is a very good agreement between prediction and experiment. This indicates that predictions of the signal level at one frequency based on the measurements at an other frequency is possible using the propagation model.

At the millimetre wave frequencies the signal fluctuations were sometimes very large, specially with increasing duct height.

## V.  CONCLUSIONS

Measurements of the propagation at the six radar frequencies for the over the horizon situation at the Atlantic ocean coast have shown a significant enhancement of the received signal level by evaporation duct effects. For the used geometry these enhancements are the strongest at 10.5 and 16 GHz with average values of about 18 dB.

Short-term comparison of measurement results with theoretical model predictions does not show very satisfactory results. This is mainly caused by the inaccuracy of the calculated duct height necessary for the propagation prediction model.
The deviations of the calculated duct height show a relation to the atmospheric stability condition.

The inaccuracy of the calculated duct height and the very fast signal fluctuation for high ducts make accurate predictions at millimetre wave frequencies at the over-the-horizon situation impossible.
At centimetre wave frequencies predictions with an accuracy of a few dB should be possible by applying an improved duct height calculation method or a more accurate duct height obtained in an other way.

1         INTRODUCTION

The propagation subgroup of NATO AC/243 (Panel3/RSG8) has conducted a measurement campaign in Lorient, France in the autumn of 1989. A total of 52 days of propagation data together with meteorological data were collected.
The participating nations and research institutes were: CELAR from France, FGAN from Germany, NCCOSC and NRL from the USA and TNO-FEL from the Netherlands.

The purpose of this measurement campaign was to get a deeper understanding of the electromagnetic wave propagation low above the sea, at horizon and over-the-horizon situations. This is of specific interest for the defence of warships against attacks by sea-skimming missiles. In this kind of situation the influence of ducting plays an important role.

This report only deals with the study based on the Dutch contribution to the campaign, the propagation data of six links in the frequency range from 3 to 94 GHz. The first part of the report is concerned with the propagation theory and the description of propagation models. This is followed by a description of the measurements. The measurement results are analysed in chapter 7. The specific meteorological condition and resulting duct situations during the campaign are described in 7.1. The next chapter contains a comparison of the signal propagation for the different frequencies and a comparison between the measured propagation and the model predictions. An extended analysis of the quality of the model predictions is described in chapter 7.3. Chapter 7.4 presents case studies describing different types of propagation, which prevailed during a number of days.

## 2 BACKGROUND

The propagation of electromagnetic (EM) waves through the atmosphere is influenced by the composition of the atmosphere. For a theoretical situation with a transmitter and receiver in free space, the path loss between the two antennas will be caused by the spatial extension of the radiated electromagnetic field. This theoretical attenuation is called the free space loss. For a terrestrial path, the propagation will also be influenced by the presence of the earth and the atmosphere. These influences are not constant in time because the earth reflection and blockage can change. For example at sea the height of the waves change, and the atmosphere changes as a result of meteorological and climatological circumstances.

This report presents a study about the influence of the atmospherical refraction on the propagation of EM signals in the radar frequency spectrum in a terrestrial just over-the-horizon situation at sea. In this situation the gradient of the refractivity in the lower part of the troposphere plays a role [2]. The refractivity on every place in the troposphere is dependent on the pressure, temperature and relative humidity of the air according to the formula:

$$N = 77.6 * p/T + 3.73 * 10^5 * (e/T^2)$$

with the ambient water vapour pressure e defined as

$$e = e_s * (RH/100).$$

In these formulae are:

- $N$ = refractivity
- $p$ = air pressure in mbar
- $T$ = air temperature in K
- $e$ = ambient water vapour pressure in mbar
- $e_s$ = saturated water vapour pressure in mbar, this is a constant for a given air temperature.
- $RH$ = relative humidity in %

Gravitation, the gas law and thermodynamic laws play an important role in the change of the refractive index with height. The water vapour pressure and air pressure normally decrease exponentially with height, while the air temperature decreases linearly with height.

## 2.1          Description of the atmosphere

Under normal circumstances we can consider the change in refractive index from the earth to about 1 kilometre height as linear. Considering the changes in atmosphere with height all over the world, a standard atmosphere is defined. The standard gradient of refractive index is characterized by a decrease of 39 N-units per km. To simplify calculations with EM wave refraction based on this world average gradient, the earth's radius is sometimes adapted. When the earth's radius in the calculations is replaced by an effective earth radius of 4/3 times the real value, the EM waves can be considered to travel in straight lines.

Of course the refractivity gradient varies with meteorological conditions. Gradients between -79 and 0 N/km are referred to as normal [3], and the standard case with a gradient of -39 N/km is called the diffraction situation. Gradients below -79, causing electromagnetic waves to bend even more towards the earth, are referred to as superrefractive. When the electromagnetic waves are bent towards the earth following a radius of curvature smaller than that of the earth, we call this a trapping condition. When the N-gradient becomes positive, the electromagnetic waves are bent away from the earth's surface. This is called a subrefraction situation.

Because the trapping situation is important in examining the effects of refractive gradients upon propagation, a modified refractivity, defined as $M=N+157*h$ for altitudes h in km, is often used instead of refractivity.

Table 1 presents the relation of N and M gradients to refraction, while figure 1 illustrates the wave paths for various conditions pictured on an earth with a 4/3 effective radius.

Table 1:       Relation of N and M gradients to refraction.

|  | N-gradient | M-gradient |
|---|---|---|
| Trapping | <= -157 N/km | <=0 M/km |
| Superrefractive | -157 to -79 N/km | 0 to 79 M/km |
| Normal | -79 to 0 N/km | 79 to 157 M/km |
| Subrefractive | >0 N/km | >157 M/km |

## 2.2    Ducting

In case of a trapping situation, the radius of curvature of a wave becomes smaller than that of the earth. This means that the wave is bent towards the earth and will either be reflected at the surface or enter a region with an other refraction condition and be refracted back upwards to re-enter the region with the trapping condition again. This type of propagation effect is called ducting, and the common term for this confinement region is a "duct" or tropospheric "waveguide". The electromagnetic energy is trapped in the duct layer, but it should be noted that some of the energy is leaking from this duct because there is no real reflection at the boundaries. This also means the transmitter and receiver do not have to be in the duct layer to observe influence on the signal propagation.

The strength of the trapping within a duct layer decreases rapidly when the angle between the direction of propagation of the electromagnetic waves and the duct layer increases.

The amount of energy trapped in the duct layer is strongly influenced by the frequency of the electromagnetic waves . In general for the lower frequencies thicker ducts better support trapping. At the higher frequencies the propagation mode within the duct can change with increasing thickness.

A duct can arise under different meteorological conditions. Dependent on the shape and height of the duct we can classify it into four types. The idealized shapes are depicted in figure 2.
- When the base of the duct is situated above the earth's surface, the duct is referred to as an elevated duct (figure 2a).
- When the base of the elevated duct is partially formed by the surface of the earth in the way as depicted in figure 2b, the duct is referred to as a surface-based duct.
- When the trapping layer starts at surface level, the duct is called a surface duct (figure 2c).
- A special type of surface duct is the evaporation duct.
This world-wide occurring type of duct is nearly permanent present at the marine boundary layer, the coupling region between the free atmosphere and the ocean.

In practical situations a mixture of two types of ducts is not unusual. Especially above the sea, a surface-based duct or elevated duct normally comes up in combination with an evaporation duct.
The evaporation duct is created by a decrease of humidity with height immediately adjacent to the sea-surface. The characteristic profile of the humidity caused by the evaporation of sea water is

responsible for the specific log-linear shape of the modified refractivity profile as depicted in figure 2d. The transitional point where trapping changes in superrefraction (M-gradient = 0), is called the evaporation duct height.

The duct height is dependent on the temperature of the sea-water and the wind speed, air temperature and humidity of the free atmosphere above the sea surface. It is a good approximation to describe the evaporation duct profile solely by the duct height.

For the experiment described in this report, the duct is calculated from the sea temperature and the wind speed, humidity and temperature of the air, measured at a few meters above the sea surface, using a duct height model.

## 3        USED MODELS

In this experiment, the transmitter-receiver path stretched out to, and just over, the horizon, dependent on the tide situation. In these situations the evaporation duct is the most important propagation mechanism.

There are different models to calculate a propagation prediction from meteorological data. Every theoretical propagation prediction is executed in two stages.

In the first stage a model is used to predict the duct height from the meteorological observations. This duct height is a measure for the atmospheric refraction profile.

In the second stage of the prediction the propagation model is used to determine the influence of the atmosphere on the electromagnetic wave propagation. With the duct height as input a propagation loss is calculated for the specific transmitter-receiver (or radar-target) set-up.

There are different models available for both the duct height and the propagation loss calculation. The used models will be shortly described.

### 3.1        Duct height model

It seems to be very difficult to obtain the evaporation duct profile directly from refractivity measurements [4]. The most reliable method to get this information is by using a duct height model. These models make use of a "bulk" measurement method based on the Monin-Obukhof [5] boundary layer theory. This means that the duct height is calculated from four input variables. These are the sea water temperature and the air temperature, wind speed and relative humidity measured at a fixed height above sea level (mostly about six metres).

We can distinguish two meteorological conditions, important for the calculation of the duct height. Dependent on the air-sea temperature difference, the atmosphere is called stable or unstable.

When the sea temperature is higher than the air temperature, the atmosphere is in a thermally unstable condition. This always creates an evaporation duct situation with a duct height that is not very sensitive to small changes in temperature, wind speed or humidity. At open sea in the absence of advection, the marine boundary layer is typically slightly unstable due to the different heat capacities of air and water.

A thermally stable condition, indicating an air-sea temperature difference that is positive, is most of the time caused by land induced effects or by advection. This condition can create higher

evaporation duct heights than the unstable case, but can also result in the absence of ducting if the air temperature becomes muc; warmer than the sea temperature. The duct height in the stable case is more sensitive to small changes in the meteorological variables.

A measure for this sensitivity is described by the bulk Richardson number [4] calculated by:

$$Rib=97.66*h1*(ta-ts)/(273.2+ta)*ws^2$$

With the air (ta) and sea (ts) temperature in degrees centigrade and the wind speed (ws) in metres/seconds. The height h1 presents the height of measurement of the air temperature and wind speed, in metres. A lower value of Rib indicates a more reliable duct height prediction. This is also the case for the thermal unstable condition. A more negative figure indicates a better accuracy of the calculated duct height.

Conditions of thermal stability with bulk Richardson's numbers exceeding 0.1, are referred to as critical. A reliable duct height calculation for such a critical condition is impossible.

The difference between duct height models mainly manifests itself in the calculation of stable atmospheric conditions.

The model used in this report, called the Paulus formulation [4], is chosen from the available models after a comparative performance test using some of the collected data.

It should be notified that the model only accounts for evaporation ducts.

For the thermal stable condition created by a warm lower humidity airflow that overlays cooler water, it is possible that apart from an evaporation duct, a surface-based duct arises by the temperature inversion above the boundary layer. In this mixed duct situation, the propagation would likely be dominated by the stronger surface-based duct. This situation can easily take place at the propagation path at Lorient because of the vicinity of the coast. We should therefore be careful in the judgement of the stable cases.

3.2        Propagation-loss model

The propagation loss predictions in this report are calculated with the PCPEM model [1]. This software package runs on a personal computer fitted with a transputer processor card. It uses the parabolic equation model calculation to obtain a two dimensional presentation of the path loss in a selected range and height area.

Input to the model are the specifications of the transmitter like the frequency, polarization, height, beamwidth and elevation of the antenna. To describe the propagation medium, the absorption parameters are derived from given air pressure, humidity and temperature, and the sea state is derived from a given wind speed. For this application, PCPEM derived the refractivity profile from the duct height separately calculated with the Paulus model.

The PCPEM model was the first commercially available personal computer based propagation model without frequency limitation for this experiment. Because of the use of the parabolic equation it was possible to do predictions for 94 GHz signals. But even with the use of the transputer card, an accurate calculation at a high frequency can take a few minutes.

An other propagation model used for this experiment is the Engineer's Refractive Effects Prediction System (EREPS) [3].

This is a system of individual stand-alone computer programs that have been designed to assist an engineer in assessing electromagnetic propagation effects of the lower atmosphere on radar systems.

These programs are very user friendly and produce very clear graphical outputs, but the program for propagation predictions under ducting conditions has its limitations for the higher frequencies. A very useful EREPS program is the Surface Duct Summary (SDS). This displays an annual climatological summary of evaporation duct, surface duct, and other meteorological parameters for a selected 10 degree latitude by 10 degree longitude square of the earth's surface. Figure 3 shows the surface duct summary of the Lorient environment. The statistics present the average annual occurrence of evaporation ducts in two meter intervals based on years of meteorological measurements.

4        EQUIPMENT DESCRIPTION


4.1        Propagation equipment

The Dutch contribution to the measurement campaign consisted of six well calibrated propagation sets. They operated at 3, 5.6, 10.5, 16, 35 and 94 GHz, and therefore represented the most important radar bands. Using the old band designations, the measurements were performed at respectively S, C, X, Ku, Ka and W- band. The antenna polarisation of all the sets was horizontal.


The sets were specially built or adapted at the FEL-TNO laboratory to fit the specifications necessary for the Lorient propagation path. Parts of the 3 and 16 GHz sets where borrowed from respectively, the Naval Command Control and Ocean Surveillance Center (NCCOSC) in San Diego, California, and the Naval Surface Warfare Center (NSWC) in Dahlgren, Virginia both in the USA. The transmitter and receiver of the 94 GHz propagation set were also borrowed from NCCOSC.

The specifications of the propagation sets are listed in table 2.

Table 2:      Propagation equipment specifications.

| | Propagation set | S-band | C-band | X-band | Ku-band | Ka-band | W-band |
|---|---|---|---|---|---|---|---|
| **T** | Frequency (GHz) | 3.008 | 5.65 | 10.5 | 16 | 34.72 | 94 |
| **R** | | | | | | | |
| **A** | Output Power (dBm) | 17.6 | 20.3 | 24.9 | 17.7 | 15.2 | 22 |
| **N** | | | | | | | |
| **S** | Antenna Type | 1 m | 1 m | 35 cm | 1.2 m | 40 cm | 23 cm |
| **M** | | PARABOLIC | PARABOLIC | LENSHORN | PARABOLIC | PARABOLIC | LENSHORN |
| **I** | Antenna Gain (dB) | 27.2 | 33.3 | 26 | 43.9 | 41 | 43 |
| **T** | | | | | | | |
| **T** | -3dB beam width (degr) | 7 | 3.7 | 8 | 1.2 | 1.4 | 1 |
| **E** | | | | | | | |
| **R** | | | | | | | |
| **R** | Input Sens. (dBm) | -40 to-110 | -15 to-105 | -30 to-105 | -20 to-100 | -30 to-120 | -35 to-110 |
| **E** | | | | | | | |
| **C** | Antenna Type | 1 m | 1 m | 1 m | 1.2 m | 40 cm | 23 cm |
| **E** | | PARABOLIC | PARABOLIC | PARABOLIC | PARABOLIC | PARABOLIC | LENSHORN |
| **I** | Antenna Gain (dB) | 27.2 | 33.3 | 40 | 43.9 | 41 | 43 |
| **V** | | | | | | | |
| **E** | -3dB beam width (degr) | 7 | 3.7 | 2 | 1.2 | 1.4 | 1 |
| **R** | | | | | | | |

Every transmitter consisted roughly of a temperature stabilised CW source followed by an isolator. In the receivers the RF power was mixed down to an IF frequency using a stable and in some cases signal locking source. The IF signal was fed through some filters to a logarithmic amplifier and detector buffered by a video amplifier.

The transmitters and receivers are connected to a parabolic or lenshorn antenna. The antenna is built in the box with the equipment or mounted on the pedestal with the transmitter or receiver. Attached to every antenna or box with a built-in antenna is an adjustable telescopic sight mounting.

The relationship between video output voltage and RF power was determined in a measurement set-up with the transmitter and receiver coupled to each other by calibrated variable attenuators. During this measurement the sets were also tested on thermal stability.

After the campaign these measurements where repeated to guarantee the reliability of the data collected during the campaign. It can be concluded that all data has an accuracy of within 3 dB total variation.

Before the campaign every propagation set was set up on a far field antenna measurement range to align the telescopic sight with the electrical boresite of the antenna. This measurement is also used to link the RF power- video voltage relation to real path losses.

During the installation of the equipment in France, the propagation sets were optically aligned with the use of the telescopic sight and a theodolite. Because the other side of the propagation path was optically not visible, the antenna azimuth alignment was carried out using some visible points with well known coordinates and the theodolite. The antenna elevation was set to the horizon at average tide with the telescopic sight.

During the measurement campaign, path losses were recorded by an HP computer with built-in AD-converter. Every ten seconds the six video voltages were measured simultaneously and written to disk every hour.

Figure 4a shows a photo of the transmitters installed at the Quiberon site. From right to left this are the 3 GHz, 5.6 GHz, 10.5 GHz, 16 GHz and the 94 GHz transmitter on top of the 35 GHz transmitter. The box on the tripod on the left of the photo is a French 36 GHz transmitter. Figure 4b shows a photo of the receivers, also in the same order, with the 3 GHz receiver on the right and the 94 GHz receiver top left.

The registration equipment was accommodated in the shelter next to the receivers.

4.2        Meteorological equipment

The most important meteorological data necessary for the propagation loss predictions was obtained from a weather buoy of the type NEREIDE XM25. It was anchored at a position of 47° 36' N latitude and 3° 15' W longitude, which was approximately halfway the path (see figure 5). It measured air pressure, air temperature, relative humidity, sun radiation, wind speed, wind direction and water temperature. Table 3 lists the specifications of the sensors on the buoy.

Table 3:     Specifications of the buoy sensors.

| parameter | accuracy |
|---|---|
| wind speed | 5 % of value |
| wind direction | 10 ° |
| water temperature | 0.1 ° C |
| air temperature | 0.1 ° C |
| relative humidity | 3 % |
| air pressure | 0.5 hPa |
| solar radiation | 1 % of value |

The water temperature was measured at a depth of 0.4 metres, while all the other sensors were located at a height of 4.5 metre above sea-level.

Meteorological stations were set up at each end of the propagation link. Their data is only used for a rough check on the buoy functioning. because they were not installed in a way to represent the open sea conditions.

The tide specifications necessary for the propagation prediction was measured at a weather station in Port-tudy, some kilometres from the path. These every hour registered values were accurate enough to describe the slow tide variation.

The observations of three weather stations in the surrounding of the path are used to get an overall idea of the weather condition. The used observations are the cloudiness and visibility registered for every 3 hour period, and the rainfall, registered as duration and total amount of rain for a period of 6 hours.
Although the data is not measured very frequently and not close to the path, it can still be used to verify a possible influence on the propagation data in periods with heavy rainfall and extremely low visibility.

## 5 PROPAGATION PATH

The experiment was conducted along a 27.7 km propagation path located near Lorient at the Atlantic Ocean coast of France. The selected sites with the transmitters at Quiberon and the receivers at Gâvres, both situated on a peninsula, should be representative for Atlantic Ocean conditions. Figure 5 shows a map of the path.

Most of the transmitters were located at a height of about 11.4 m above zero sea level. The actual sea level at the sites varied sinusoidal round 3 m above zero sea level with an amplitude that can vary between 0.75 and 2.5 m. This results in an effective transmitter height between 5.9 and 10.9 m with an average of 8.4 m. The effective receiver height varies between 7.9 m and 12.9 m with an average of 10.4 m. Table 4 lists the exact heights of the transmitters and receivers at average tide.

Table 4: *Transmitter and receiver heights at average tide.*

| PROPAGATION SET | TRANSMITTER HEIGHT | RECEIVER HEIGHT |
| --- | --- | --- |
| 3 GHz | 8.37 m | 10.41 m |
| 5.6 GHz | 8.37 m | 10.41 m |
| 10.5 GHz | 8.35 m | 10.50 m |
| 16 GHz | 8.36 m | 10.40 m |
| 35 GHz | 8.23 m | 10.27 m |
| 94 GHz | 9.25 m | 11.29 m |

The transmitter-receiver propagation link was most of the time over the horizon. At low tide the path was within the radar horizon. This resulted in a large influence on the propagation loss that must be accounted for, making the comparison of measured data with predictions much more complicated.

## 6 PROPAGATION PREDICTIONS

The variable parameters accounted for in a propagation prediction are the tide, and the duct height calculated by the duct height model. The resulting path loss value is corrected for atmospheric attenuation due to the humidity of the air, which has a major influence for the higher frequencies.

Because a direct model prediction for every 10 minutes of meteorological data would take too much time, the path loss is derived from a pre-calculated table for every propagation set. Every table consists of path loss values calculated as a function of the duct height and the sea level, assuming an average wind speed of 10 m/s, producing an rms waveheight of 0.5 metre. The prediction is determined by a double linear interpolation in the table.

The influence of the duct height on the path loss of the six propagation links for average tide level is presented in figure 9a, while the influence of the tide on three of the links is presented in figure 9b.

Figures 6a to 6f show a few contour plots calculated with PCPEM which have been used to get path loss values for the table. The contour plot presents the path loss by a different colour for every 5 dB interval for a two dimensional range-height area. The height in the plot is taken from the actual sea level, while the 0 km range represents the place of the transmitter. With the PCPEM program we can accurately read out the path loss on every place in the area.

For example at S-band (figure 6a and 6b), the receiver is situated at a range of 27.7 km and a height of 10.4 metre above sea level at this average tide situation. In figure 6a the standard atmosphere situation (0 m duct height) is depicted. For the given range and height we can read out a path loss of 153.5 dB. This is called the diffraction value because of the standard atmosphere situation. In case of a 20 meter high evaporation duct as depicted in figure 6b, we can read out a path loss of 132.4 dB. This means a signal improvement of more than 20 dB.

By comparison of the figures 6a and 6b we can see that the structure is bent to the earth under the ducting situation.

Figures 6c to 6f show that for the higher frequencies the entire multipath lobing structure seems to be bent towards the earth under ducting influence. This results in a successive increase and decrease of the path loss with increasing duct height. This relation does not always produce a

regular loss pattern due to the multimode propagation within the duct for the higher frequencies. In figure 6d this is clearly visible.

An other way to look at this ducting influence is by means of the range plots. These figures present the path loss versus range at the height of the receiver. The range plots for different duct heights are presented in figure 7a for 3 GHz and in figure 7b for 35 GHz, both for average tide situations. Every duct height situation is presented by a different coloured line in the plot.

For the S-band (3 GHz) configuration of figure 7a we can see that the path loss is regularly decreasing with duct height for the 27.7 km distance.

At Ka-band (35 GHz) in figure 7b, this regularity is disturbed by the multipath interference. For the diffraction situation (violet line, 0 m duct) the receiver at 27.7 km is not in the interference region, but the multipath interference zeros are stretched out over the path for the higher duct heights.

Figure 9a clearly reflects the influence of the shifting interference nulls with duct height for the millimetre wave frequencies. The height of the transmitter and receiver is also relevant for the multipath interference, as indicated in figure 9b.

A propagation mechanism other than the evaporation duct, is the surface-based duct (SBD). This type of trapping layer arises at certain conditions and extends from an altitude higher than the evaporation duct till several hundreds of metres. Modelling of the SBD requires profile measurement instead of the available bulk meteo measurements. Since the SBD did influence the measurements, it is good to consider the effect of this type of ducting.

One feature of surface-based ducts is the skip zone which extends from the transmitter to a distance which depends on the surface-based duct height. In the skip zone the path loss does not depend on the surface-based duct.

Figure 8 shows a range plot for the 3 GHz configuration at average tide level, with the propagation characteristics at evaporation duct and surface-based duct situations. The propagation loss under diffraction and at a maximum evaporation duct enhancement are given by the two black lines. For different evaporation duct heights the curves are situated between these limits, like in figure 7a.

The influence of surface-based ducts of different heights is illustrated by the coloured lines. We can see that a SBD higher than 75 metre has no effect on the propagation loss because the receiver is situated in the skip zone.

In a combination of the two types of duct the effect of surface-based ducts with heights between 40 and 75 metre depends on the evaporation duct height. The presence of a SBD height smaller than 40 meter for the figure 8 configuration can easily be recognised because the enhancement exceeds the maximum enhancement value of an evaporation duct. The SBD influence for the different sets depends mainly on the transmitter and receiver heights; the frequency has no noticeable influence.

According to the annual surface duct summary of figure 3 surface-based ducts lower than 75 metre are possible in this area.

## 7  EXPERIMENTAL RESULTS

A consecutive period of 52 days (23 September to 13 November 1989) with both reliable propagation and meteorological buoy measurements collected during the Lorient campaign, was selected for further data analysis.

### 7.1  The meteorological data

Figures 10a to 10c show graphical presentations of the most important meteorological data for one day (based on Greenwich Mean Time). These parameters are used for the calculation of the duct height and the prediction of the path loss and for the exclusion of data in statistical comparisons.

The presented air and sea temperature, relative humidity, wind speed and direction, air pressure and solar flux are measured by the buoy located halfway the propagation path.

The wind direction in the plot is presented for every hour by the arrows on top of the wind speed plot (they point in the direction the wind came from). The solarflux plot presents the intensity of the sunlight, with a maximum value of 700 W/m$^2$ at noon of a sunny day at the begin of autumn. The other buoy data is presented by a line through all the 10 minutes observations.

The tide level variation is measured at a meteorological coast station near the path. This level varies about sinusoidal round the three meter above zero sea level point with a slowly changing amplitude.

The meteorological observations presented in the bottom left picture are obtained from weather stations in the neighbourhood of the measurement path. They therefore do not necessarily represent the actual situation at the path. The cloudiness and visibility are determined over 3 hour periods. The first is classified on a scale of 0 to 8 and presented by 0 to 8 horizontal lines. A clear sky is indicated by the absence of a line while 8 lines indicate heavy cloudiness. The visibility is indicated by two arrows connected by a line. If the arrows cover the entire 3 hour scale, the visibility is 2240 metre or more. In heavy fog conditions (0 metre visibility), the points of the arrows touch. The rainfall recorded in 6 hour periods is represented by a water-butt. The width represents the rain period in hours on the right scale, and the contents indicates the average rainfall, with a full butt representing 5 mm rain/hour.

The duct height presented by the bottom right picture is directly calculated with the Paulus formulation from the air and sea temperature, wind speed and relative humidity in the figure.

### 7.1.2 Meteorological conditions during the campaign

In figure 10a we can see that the air temperature exceeds the sea temperature during the day-time. This increase of temperature was a frequently returning phenomenon, but no general rule during the campaign. Figure 11 is a statistical presentation of the four input parameters for the duct height calculation.

The air temperature statistics show a gaussian distribution with an average value of 16 degrees.

Since the measurements were performed in the autumn, there was a slow decrease of the ocean temperature over the period, from about 17.5 degrees at the start of the campaign, till 13 degrees on the last day. This resulted in the sea temperature distribution of figure 11b. At the start of the campaign the weather was mild, succeeded by periods with heavy fog and some tempestuous periods with a lot of rain and severe storms. The wind speed statistics show the relatively frequent occurrence of the high wind speeds. The humidity above the sea surface is always high, but the large amount of fog periods contributed to the unusually high occurrence of 90 to 100 % humidity in figure 11c.

Important to the duct height prediction is the difference between the air and sea temperatures. Figure 12 presents this statistically for the Lorient campaign. Stable conditions (air temperature higher than sea temperature) occurred in total for 72.2 percent of the time. During 14.8 percent of the time the Bulk Richardson number exceeded the critical 0.1 value, which means that the duct height was impossible to calculate. The unusual high percentage of stable conditions can be explained by the direction of the wind which was most of the time from the North, blowing air from the mainland over the colder sea.

### 7.1.3 Evaporation duct height statistics

A statistical presentation of the duct heights calculated with the Paulus formulation is presented in figure 13. The total percentage of occurrence of duct heights within a one metre interval for the entire measurement period is presented in the column before the graph, and presented by the full length of the bar in the graph. To make a distinction between the first and second half of the measurement period, the bars are split up in two parts.

The percentage of the first half of the measurement period (23 September to 18 October) is presented by the length of the light shaded bars on the left, and the second half (19 October to 13 November) by the length of the dark shaded bars.

Remarkable is the large amount of calculated duct heights lower than one meter in figure 13. This comprised 24.1 percent of the time, of which 3.8 percent occurred in the first part of the period and 20.3 percent in the second part.
A deeper study of these duct heights revealed that only a few days in the second part of October were responsible for this data.
During this period with a lot of fog, there was most of the time no duct. At that time, the atmosphere was stable with an air temperature more than 1.5 degree higher than the sea temperature and a very high relative humidity of more than 94%.

When we compare the entire graph to the annual duct height summary of the EREPS program in figure 3, we see an entire different shape of the figures. Exclusion of the calculated duct heights when the Bulk Richardson number exceeded 0.1 does not appreciably change the statistics. Looking at the duct height statistics of the first and second half of the measurement period we can observe a large difference between the shapes of the statistics.
The first half of the period shows a resemblance to the annual duct statistic, while the second half of the period certainly does not.
This indicates that the campaign can not be considered representative for the entire year period.

7.2        Propagation measurements

The video voltages of the six receivers were measured every 10 seconds, which results in 8640 values per day for every frequency. These values were transferred into path losses using the calibration tables.
The figures 15 a, b and c show for three different dates the path loss of the six sets presented in a day-plot. Every 10 seconds measurement is indicated by a dot. This way of presentation gives a good impression of the signal fluctuations. At the higher frequencies we can see an increase of the fast signal fluctuations when the lower frequencies are enhanced by ducting conditions.

7.2.1        Long-term statistics.
For the statistical analysis of the signals the values are averaged to get one value for every 10 minutes. A measure for the influence of the duct on the signal is the enhancement factor. This is

defined as the factor of improvement (positive factor) or deterioration (negative factor) of the signal strength compared to the diffraction value. The diffraction value is the path loss when there is no duct (standard atmosphere) and is in this case dependent on the tide and, to a lesser degree, on the atmospheric attenuation. For the used frequencies, table 5 enumerates the free space loss and diffraction values for different sea levels. The high and low tide values in the table are obtained for the extreme tide variation cases with 2.5 metre deviation from the average tide. The diffraction value is calculated for an average weather condition with an absolute humidity of 7.5 g/m$^3$. The absorption per g/m$^3$ for this path is given in the last column of table 5.

Table 5:     Propagation losses for the Lorient path.

| frequency (GHz) | free space loss (dB) | diffraction loss (dB) | | | atmospheric absorption dB/g/m$^3$ |
|---|---|---|---|---|---|
| | | low tide | avg. tide | high tide | |
| 3 | 130.9 | 148.6 | 153.5 | 159.5 | 0.002 |
| 5.6 | 136.4 | 152.0 | 157.3 | 164.0 | 0.007 |
| 10.5 | 141.7 | 155.4 | 161.4 | 169.0 | 0.027 |
| 16 | 145.4 | 158.0 | 164.4 | 172.4 | 0.093 |
| 35 | 152.2 | 163.0 | 169.6 | 178.1 | 0.288 |
| 94 | 160.8 | 174.7 | 182.1 | 189.6 | 1.684 |

Figures 17a through 17f show the enhancement factors measured during the campaign.

The bell-shaped peak in every figure suggests a frequently occurring duct height, in contradiction to the duct height statistics of figure 13. At 5.6 to 16 GHz we can clearly see a higher occurrence of 0 dB enhancement factors compared to adjacent values. This corresponds to the large amount of non ducting situations in the duct height statistics of figure 13.

The low enhancement factor values occurring at the higher frequencies are mainly caused by attenuation due to rain or fog. This appears from the high correlation of these enhancement factors with the rainfall and visibility information of the meteo observations. The scarcely present subrefraction cases also contribute to the very low enhancement factors.

From a comparison of the six frequencies we can see that the 10.5 and 16 GHz signals are the most enhanced, with the highest occurrence of values round 18 dB. Together with the PCPEM predictions of figure 9a we can find some explanations for the behaviour of the different frequencies. The increase in enhancement factor with frequency up to 16 GHz indicates a low duct height. The modal occurrence of an enhancement factor of about 18 dB for both 10.5 and

16 GHz indicates a regular occurrence of duct heights round the six metres. At the higher frequencies (35 & 94 GHz) the maximum overall enhancement at these lower duct heights is smaller and the signal fluctuation as a function of the duct height and tide becomes relevant.

It is important to realize oneself that a different height of the transmitter or receiver can create different situations. The long-term propagation statistics are useful in radar system design and communication link performance research.

### 7.2.2 Short-term comparison of measured and predicted path losses

In an operational radar situation it is important to have an accurate short term propagation prediction. For every 10 minutes of the 52 days period of the campaign, the propagation predictions were calculated using the meteorological data and models described earlier. Figure 16 shows a graph with the curves of the measured and predicted path loss for one day. The measured signal is averaged over the same 10 minutes periods as the prediction is calculated and presented by the solid line. The predictions for this day are presented by the dotted line.

The comparisons between all measured and predicted path losses for a frequency are presented in the figures 18a to 18f. The data in the figures cover the entire measurement period. The figure on top is the scatterplot, presenting direct comparison of the predicted and measured path loss for a ten minutes period by a dot. The diagonal line in the plot indicates the ideal positions where the predicted and measured path losses are equal. A dot above the diagonal means that the predicted value is lower than the measured, and a dot below this diagonal indicates a predicted value higher than measured.

The data is distinguished into three classes, dependent on the atmospherical condition at the time of measurement. The data measured under unstable conditions is presented by green dots. The data measured under stable conditions is presented by blue or red dots, dependent on the bulk Richardson number.

Measured path losses above the clip limit, presented by the vertical line in the scatter plot, are considered to be influenced by attenuation effects that can not be corrected for. The clip-limit value is based on the highest possible diffraction value at a maximum atmospherical attenuation situation for that frequency, increased with a safety margin of 3 dB.

The higher measured path loss values are caused by heavy rainfall, dense fog or in some cases by subrefraction.

A presentation of the prediction performance is given at the bottom of the figure. In this statistical plot the deviation of the prediction from the measurement is plotted for every 1 dB measured path loss interval, and is therefore a measure for the quality of the predictions. Values to the left of the clip limit are omitted and also the stable data with a bulk Richardson number higher than 0.1, and intervals with less than 10 values are not implemented in the deviation plot.

The average deviation is calculated by the summation of the deviation (predicted-measured path loss) in the measured path loss interval, and divided by the number of data points. In the rms deviation the sign of the deviations is eliminated before summation, using the root mean square principle.

The total rms deviation value is the rms result of all individual deviation values in the entire measurement range and is a measure for the overall quality of the predictions. The deviation plot can not be considered apart from the scatterplot which provides the information about the quantity of data points in a statistical interval.

The calculations for all these deviations are performed on the dB values.

Remarkable about the scatterplots is the difference in behaviour of the data measured under the stable and unstable condition. The data of the unstable condition is concentrated on a curve above the ideal line, while the blue stable-condition points are more spread out round the ideal line. Among the red coloured stable data (14.8 % of all points) are a lot of very bad predictions, although not all these values are bad.

The average deviation values represent results on a long-term statistical base, like the sometimes used "percent occurrence graphs". Although these long-term statistics can result in very nice fits between the measured and predicted data, it does not reflect the quality of short-term predictions. When we look for example at the quality of the predictions at X-band (fig.18c) for the measured path losses between 150 and 151 dB, we can see in the scatterplot that the points are widely spread. The average deviation for this interval is nearly zero while the rms deviation is about 9 dB. For the individual short-term predictions, this means an average error of 9 dB, although a long-term statistical comparison could predict a perfect fit.

The total rms deviation is increasing with frequency, with an exception for 94 GHz. The reason for this exception is the smaller measurement range. Most of the measured values at 94 GHz are between 175 and 190 dB. The rms deviation for this 15 dB range of + or - 6.1 dB indicates a very bad prediction.

Looking at the total rms deviation numbers for all frequencies, we can conclude that the predictions are rather poor.

For example, the total rms deviation of 6.1 dB at 10.5 GHz can also be obtained with a fixed prediction value of 145 dB. The disadvantage of this one value prediction is of course the always poor predictions for the extreme signal enhancement and attenuation cases.

## 7.3 Research into the quality of predictions

The bad correlation between the propagation predictions and measurements can be caused by bad measurement data. This is unlikely because all equipment was calibrated before and after the campaign, and no appreciable difference was observed. The alignment of the antennas at the site was executed with the highest accuracy. A comparison between the Dutch 35 GHz and French 36 GHz data, and the Dutch and American 94 GHz data also confirmed the quality of the measurements.

Bad propagation predictions can be caused by the propagation prediction model, the duct height calculation model, the cooperation between these two, or by bad meteorological parameters for the duct height calculation.

### 7.3.1 Optimum-duct-height calculation

One way to check the propagation prediction model is to look at the relation between the predictions for the different frequencies, compared to the measurements. For this purpose one optimum-duct-height characteristic is calculated from the duct heights at every frequency obtained by a search for the measured path loss value in the pre-calculated PCPEM prediction table. For the low frequencies (3, 5.6, 10.5 and 16 GHz), the duct height of the path loss prediction in the PCPEM table which matches the measured path loss value is obtained. The tide level at the moment of measurement is of course taken into account in this process. As indicated in figure 9a, there are sometimes more duct heights possible for frequencies higher than 5.6 GHz. The 35 and 94 GHz data are not used in this process because they produce too many solutions (at 94 GHz for every metre) and are too sensitive for small tidal errors.

The process of calculation of the optimum duct height is graphically presented in figure 19. Every possible duct height for a frequency is presented by a coloured dash. The solid violet curve in the figure is calculated with a best fit algorithm from the duct heights for all frequencies. This optimum-duct-height curve gives the best PCPEM loss prediction averaged over all frequencies. The orange to brown curve in figure 19 shows the duct height calculated from the meteorological parameters with the modified Paulus formulation. The actual colour indicates the meteorological stability at that moment.

When we compare the optimum-duct-height curve with the duct height curve calculated from the meteorological conditions we observe a poor resemblance for some of the periods. In the unstable cases like from 0 to 8 hour and from 21 to 24 hour at 28 September we see that the duct height calculated from the meteorological data is up to about 5 metres higher. The resemblance under stable conditions is for this day a little better.

### 7.3.2    Optimum-duct-height statistics

Figure 14 presents the statistics of the optimum duct heights calculated from the path losses measured during the campaign. The measurement data is just like in figure 13 split up into two equal parts, with the first part of the measurement period presented by the light shaded bar and the second part by the dark shaded bar. When we compare figure 14 with the statistics of the duct heights predicted from the meteorological data with the Paulus model as presented in figure 13, we observe that both show a preponderance of very low duct heights of 0 to 1 metre.

Figure 14 shows a similar large difference between the first and second half of the measurement period as in the Paulus predictions. The first part shows a shape with a resemblance to the annual duct height statistics of figure 3, although the duct heights are generally lower. The second part of the period shows an almost equal occurrence of duct heights between 1 and 10 metres. The occurrence of large duct heights in figure 14 is caused by the path losses which are reduced by non-evaporation duct effects that are without exception treated by the optimum-duct-height calculation procedure as if they were due to evaporation ducts. In general the optimum-duct-height statistics show a better agreement with the annual duct statistics than those calculated from the meteorological data with the Paulus model.

Of course, is should be kept in mind that the measurement campaign only covers a part of the year, at a geographical location that can be influenced by specific land-induced effects.

The optimum duct height calculated for every ten minutes period is again used to predict the path losses for all frequencies. A comparison between this prediction and the measurements in a scatterplot as in figures 18a to 18f shows a much better correlation.

The total rms deviations for the frequencies from 3 to 94 GHz are now respectively: 2.0, 1.6, 2.6, 3.8, 6.3 and 5.1 dB instead of 5.3, 6.2, 6.1, 6.5, 7.6, and 6.1 dB. This improvement is partly logical because this method aims at reducing the difference between measured and predicted loss, but the deviations for all frequencies are improved a lot. This analysis leads to the following expectations. First, there seems room for the improvement of the meteorological model which provides the duct height. Second, because of the agreement between the predictions at different frequencies, it might be possible to apply the propagation loss model in order to use the measured performance at one frequency to predict the performance at an other frequency.

Figure 21 shows the comparison between the path losses calculated from the optimum duct height and the measured path losses at 10.5 GHz. Most of the points, and all of the points of data measured at an unstable atmosphere condition, are situated round the diagonal. The largest deviations are caused by stable atmosphere condition points at the extreme high and low path loss values. It is possible that a part of the low path loss values are caused by surface-based ducts, and that high path loss values are influenced by rain or fog attenuation or possibly by subrefraction.

### 7.3.3 Comparison of duct heights

Figure 20 shows the relation between the duct heights predicted from the meteorological data and the optimum duct heights calculated back from the measured path losses. The difference between these duct heights for every 10 minutes period is presented against the duct height from the meteorological data. The difference is calculated by subtracting the optimum duct height from the duct height predicted from the meteorological data, so a positive difference means that the duct height predicted from the meteorological data is too high.

The atmospherical condition at the time of measurement is indicated by the colour of the dots. We can see that all of the unstable predictions are too high. Most of the stable predictions are grouped around a sloping line running from -4 metre difference at 0 metre prediction from meteorological data up to about 8 metre difference at 15 metre prediction from meteorological data. The extreme negative differences are probably caused by surface-based duct enhancement cases. If we assume the optimum duct height as correct, we can conclude that the duct height calculated from the

meteorological data is not very accurate, but the error is consistent and can probably be corrected in a simple way.

It should however be realized that the duct height is only one value used to describe the entire refractivity index profile. If the assumption of the shape of this profile by the propagation model does not agree with the shape used by the duct model, this can also be a reason for inaccuracies.

7.4        Case studies

During the Lorient '89 campaign, the propagation characteristics of totally 52 days have been measured. All these days are different and there are many interesting periods, but it will be outside the scope of this report to discuss every day. Therefore three selected days with specific situations will be discussed to get an impression of the practical signal behaviour.

7.4.1        An average day with evaporation-duct enhancement

September the 28th can be considered as an average day of the first part of the measurement campaign. It gives a good impression of the effect of duct height changes on the observed path loss values. Figure 15a presents the path losses of the received signals at the six frequencies. The weather condition during that day is presented by figure 10a while figure 19 presents the calculation of the best duct height. The meteo report indicates no rain or dense fog that can lead to loss of signal during that day.

Looking at the path loss signals and the PCPEM predictions graph for average tide of figure 9a, we can almost explain the signal behaviour from hour to hour. At 0:00 hour the 10.5 and 16 GHz path losses are a little lower than those at 3 and 5.6 GHz, while the loss at 35 GHz is about 15 dB higher. This corresponds with the 5.5 to 6 metre situation of figure 9a.

In the period till 7 o'clock the duct height is decreasing to about 3 to 4 metre, indicated by the 35 GHz path loss recovering from the interference zero and the 3 to 16 GHz frequencies having path losses increasing in order of frequency.

From 7:00 hour to 16:00 hour, the duct height is increasing to about 20 metres. The measured path losses show exactly the same characteristic as the PCPEM prediction of figure 9a from 5 to 20 metre duct height.

After 16:00 hours the duct height is again decreasing to about 6 metre at midnight.

When we look at the behaviour of the 35 GHz signal during the day, we can clearly see the interference pattern of the nulls at 6 and 10 metre duct height (like at 7:45 hour and 10:45 hour),

but the signal level is getting more noisy with increasing duct height (like from 12:00 to 18:00 hours). The noisy character at higher duct heights can be observed at all frequencies, but is a lot stronger at higher frequencies. At 94 GHz we can observe some interference nulls till about 10 o'clock, but afterwards the signal looks like a noise band. Although figure 15a cannot provide this information, it has been verified that the signal may vary up to 20 dB in 10 seconds. This is according to the path loss prediction curve of figure 9a about the same as the maximum path loss variation caused by the change of the duct height. This makes a prediction at millimetre wave frequencies (35 and 94 GHz) for higher duct heights impossible.

For a reasonable path loss prediction we can derive from figure 9a that we need a duct height accuracy of at least 0.25 metre at 94 GHz and 0.5 metre at 35 GHz. In the previous chapter we have seen that even a duct height accuracy of 1 or 2 metre is difficult to obtain. It is therefore obvious that accurate predictions for the millimetre wave frequencies are impossible. For all frequencies we can observe an increase of signal fluctuations with duct height. This indicates a larger variation of the duct with increasing height.

### 7.4.2 A day with surface-based-duct enhancement

In the afternoon of 16 October (figure 15b) we have definitely a situation of surface-based ducting. Till about noon, all signals are slowly enhanced in a normal way. From 12:00 to 15:00 hour, the 3 GHz signal is suddenly enhanced with about 20 dB. The 120 dB path loss is according to figure 9a not possible with evaporation duct heights up to 26 meter, and the occurrence of higher evaporation ducts is very rare.

Figure 8 shows the effect of surface-based-ducts on the 3 GHz propagation loss. According to this figure the maximum enhancement by an evaporation duct is reached at a 30 meter duct height with a propagation loss of 127 dB, while a loss of about 120 dB is reached with a surface-based duct less than 40 meters high. The measured path loss reached this 120 dB value which indicates the surface-based-duct situation.

These surface-based-duct situations identified by low propagation loss occurred about 4% of the time during the campaign. The total percentage of surface-based duct occurrence is probably about twice as high, but the effects of surface-based ducts between 40 and 80 meters are difficult to recognize. The annual surface duct summary of figure 3 predicts an 1% occurrence of surface-based duct and an average thickness of 68 meters. The difference can be caused by the

measurement site, being more influenced by land induced effects, or is a result of meteorological effects during the campaign who are not representative for the entire year.

In the meteo report of 16 October 1989 (figure 10b) we can not find anything unusual that points to the surface-based-duct situation. We can only observe the stable condition that is always present during a surface-based-duct situation, but does not necessarily indicate a surface-based duct. The evaporation duct height in the figure, predicted by the Paulus model, shows no changes during the surface-based-duct circumstances, probably because both kind of ducts were present, but worked independently of each other on different altitudes.

### 7.4.3        A day with subrefraction

In the path loss figure (15c) of 18 October 1989 we can observe the rare occurrence of subrefraction. At the start of the day the path losses of all frequencies are almost equal to the diffraction values. Three hours later these path loss values are increased with at least 15 dB with some of the signals exceeding the input sensitivity of the receivers. This path loss increase can only be caused by subrefraction because there are no types of atmospherical attenuation that can have such an impact on the low frequencies.

The meteo report of figure 10c shows the circumstances of that day. Most remarkable is the very low visibility during that day, with an average of 400 metre for the first three hours and values ranging between 10 and 100 metre for the rest of the day. The atmosphere was stable with a small air-sea temperature difference, the wind speed low and the humidity very high, which is normal at dense fog conditions. There has been a short period with heavy rainfall between 6:00 and 12:00 hour and a period of about one hour rain between 12:00 and 18:00 hour. The effect of this rain is difficult to recognise in the path losses graph. Rain in general slightly counteracts ducting and causes more attenuation at the higher frequencies.

Weather conditions like those on 18 October, a stable atmosphere with an air temperature more that 1.5 degree higher than the sea temperature and a very high relative humidity of more than 94 % occurred a few days during the measurement period. These days are normally characterized by a predicted absence of duct and the path losses are mostly equal to diffraction values.

The subrefraction situation of 18 October is very exceptional and occurred only in a few other occasions with much less decline in signal level.

## 8        CONCLUSIONS

Measurements of the propagation at the six radar frequencies in an over-the-horizon situation at the Atlantic Ocean coast have shown a significant enhancement of the received signal level by evaporation duct effects. For the used geometry these enhancements are most pronounced at 10.5 and 16 GHz with average values of about 18 dB.

Short-term comparison of measurement results with theoretical model predictions does not show very satisfactory results. This is mainly caused by the inaccuracy of the calculated duct height necessary for the propagation prediction model. Although the duct height calculation from the meteorological data is a very difficult matter and accuracies of less then a few meter will probably never be reached, there are possibilities to improve the calculations. An extended research revealed some consistent deviations in duct height calculations for different meteorological conditions that can probably be reduced easily.

The inaccuracy of the calculated duct height and the very fast signal fluctuation for high ducts make accurate predictions at millimetre-wave frequencies in the over-the-horizon situation impossible.
At centimetre-wave frequencies predictions with an accuracy of a few dB can be possible by applying an improved duct height calculation method or a more accurate duct height obtained in an other way.

## REFERENCES

[1] Craig, K.H.; Levi, M.
PCPEM software program.
Signal Science Limited, Abingdon, Oxon, UK, 1990.

[2] Hall, M.P.M
Effects of the troposphere on radio communication.
Peter Peregrinus Ltd, London, 1979.

[3] Patterson, W.L. et al,
Engineers Refractive Effects Prediction System (EREPS).
Artech House, London, Boston, 1990.

[4] Paulus, R.A
Specification for environmental measurements to assess radar sensors.
TD-1685, NOSC, San Diego, California, USA, 1989.

[5] Monin, A.S.,Obukhov, A.M.
Basic laws of turbulent mixing in the ground layer of the
atmosphere.
Akad. Nauk. USSR, Geofiz. Inst. Tr., 1954.

G.A. van der Spek
(Groupleader)

R.B. Boekema
(Author)

FIGURES
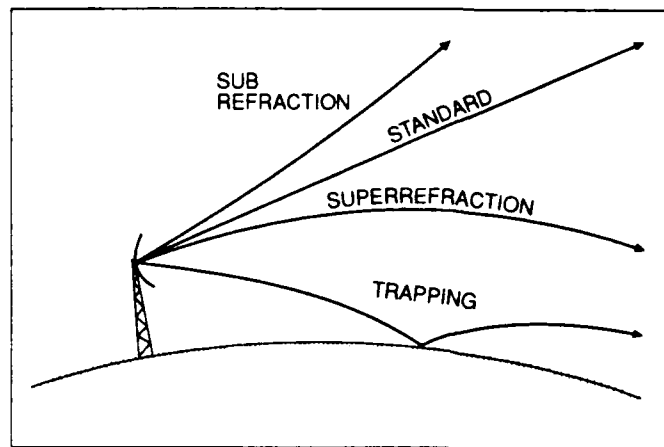


fig. 1    Wave paths for various refraction conditions depicted on an earth with a 4/3 effective radius
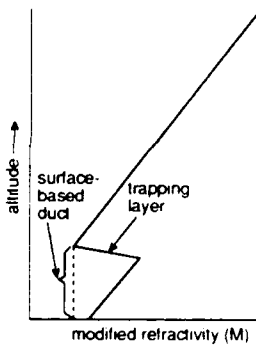


(a) Elevated duct formed by an elevated trapping layer
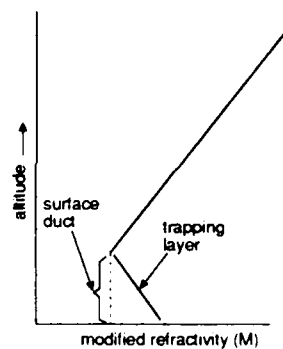


(b) Surface-based duct formed by an elevated trapping layer
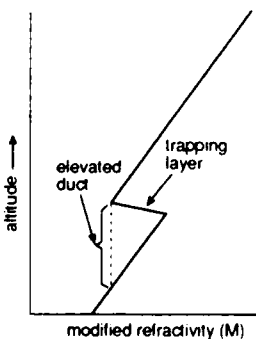


(c) Surface duct formed by a surface trapping layer
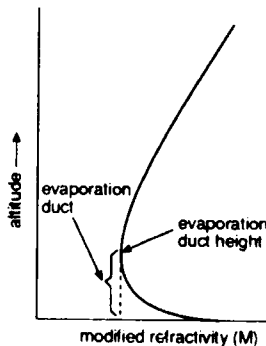


(d)    Evaporation duct formed by a decrease of
humidity immediately adjacent to the sea surface

fig. 2    Four types of duct classified by the refractivity profile

```
EVD HT        % OCCUR  0      5     10     15     20     25     ┌──────────────────┐
                                                               │      ANNUAL      │
                                                               │ SURFACE DUCT SUMMARY │
0 TO  2 m      9.8                                             └──────────────────┘
2 TO  4 m     10.4  E                                          SURFACE OBS: MS 145
4 TO  6 m     14.8  V
6 TO  8 m     17.0  A                                          LATITUDE:    40 TO  50 N
8 TO 10 m     15.7  P                                          LONGITUDE:    0 TO  10 W
10 TO 12 m    12.7  O                                          AVG EVD HT:       8.2 m
12 TO 14 m     8.9  R                                          AVG WIND SP:    15.0 KTS
14 TO 16 m     5.6  A                                          SAMPLE SIZE: 241624 OBS
16 TO 18 m     3.1  T
18 TO 20 m     1.5  I                                          UPPER AIR OBS: RS  7110
20 TO 22 m     0.7  O
22 TO 24 m     0.3  N                                          BREST/GUIPAVAS, FRANCE
24 TO 26 m     0.2
26 TO 28 m     0.1  D
28 TO 30 m     0.0  U                                          LATITUDE:        48.45 N
30 TO 32 m     0.0  C                                          LONGITUDE:        4.42 W
32 TO 34 m     0.0  T                                          SBD OCCURRENCE:    1.0 %
34 TO 36 m     0.0                                             AVG SBD HT:         68 m
36 TO 38 m     0.0  H                                          AVG NSUBS:         327
38 TO 40 m     0.0  T                                          AVG K:            1.39
   > 40 m      0.0                                             SAMPLE SIZE:      3257
```

fig. 3    Annual surface duct summary of the Lorient environment, presenting the statistics of
the percentage of occurrence of evaporation duct heights during the year.

fig 4a   Transmitter equipment installed at the Quiberon site.



fig 4b   Receiver equipment installed at the Gâvres site
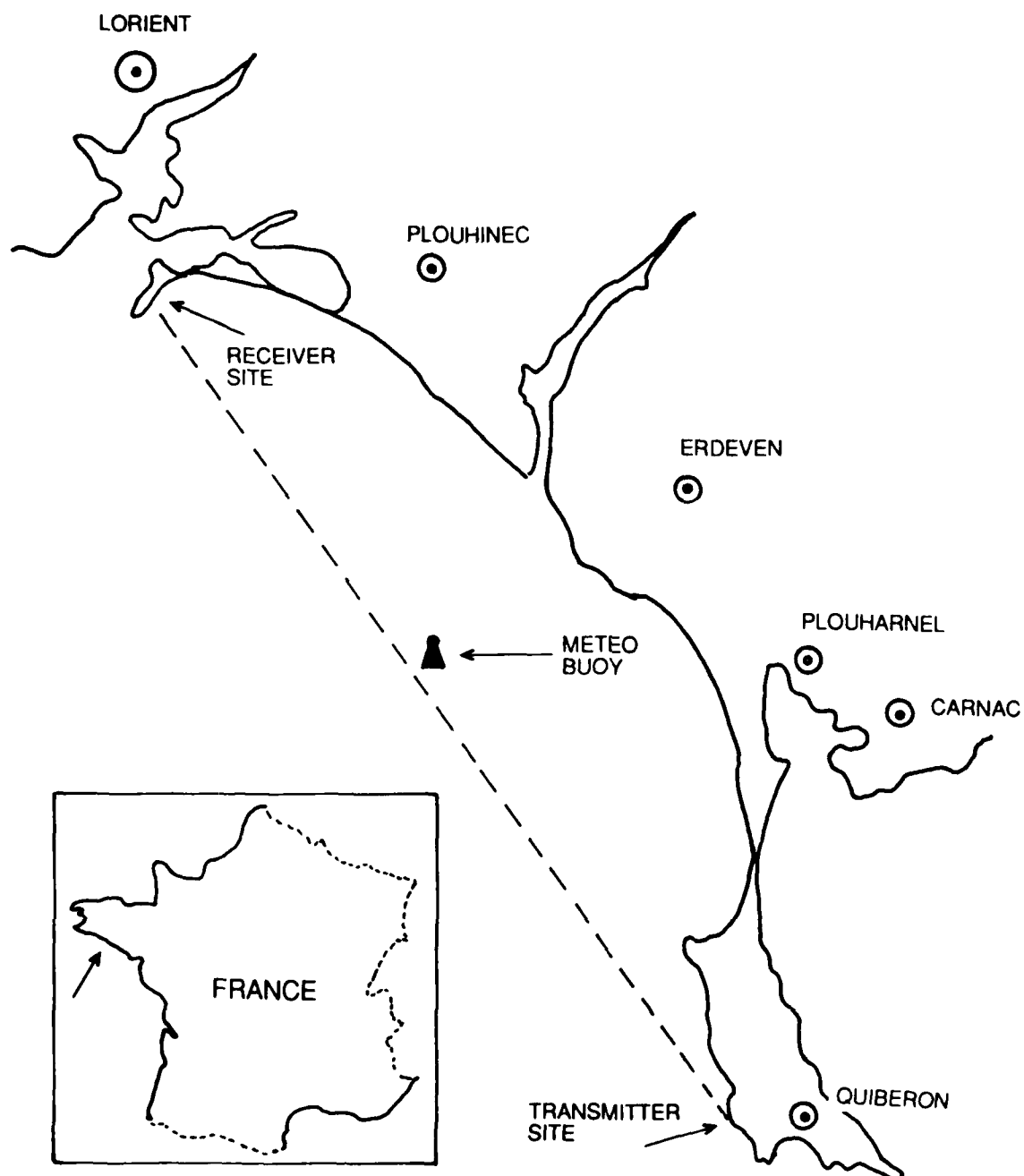
fig. 5    Map of the propagation path.
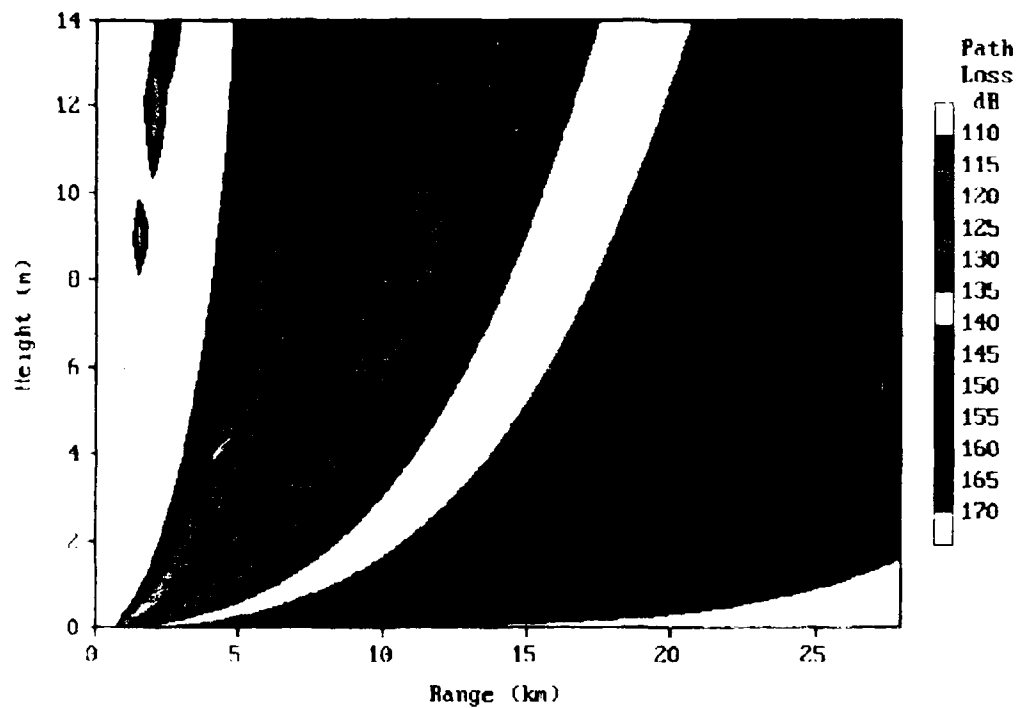
fig. 6a   Coverage diagram for the S-band configuration at average sea-level and a duct height of 0 metre.
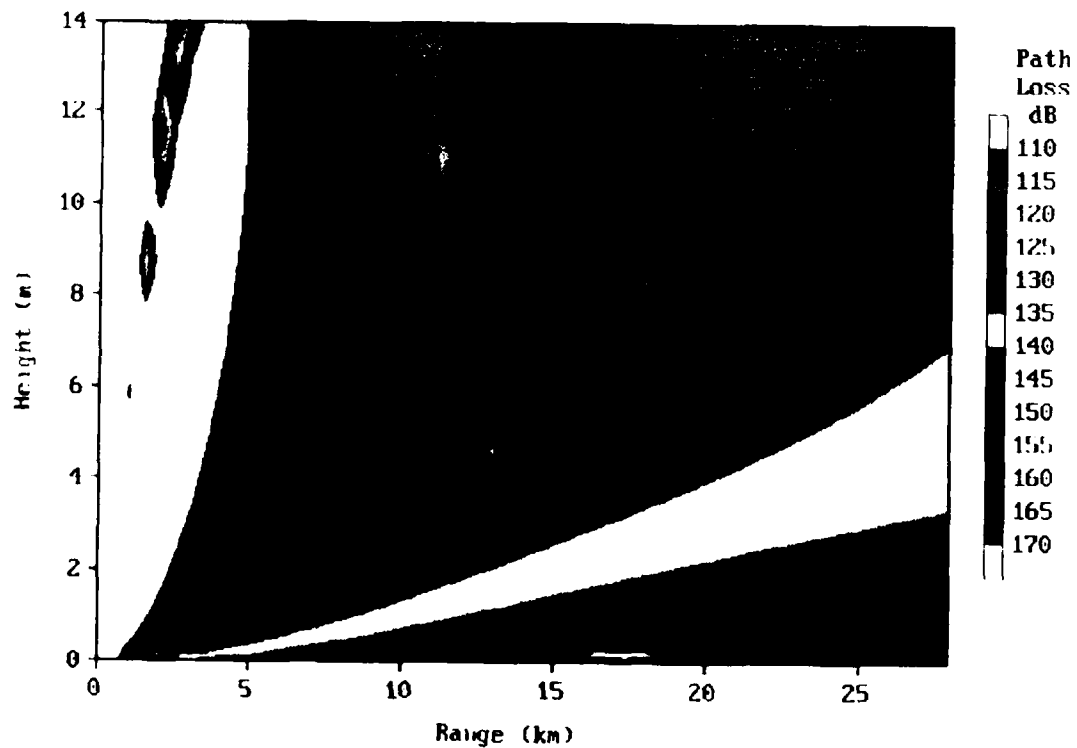


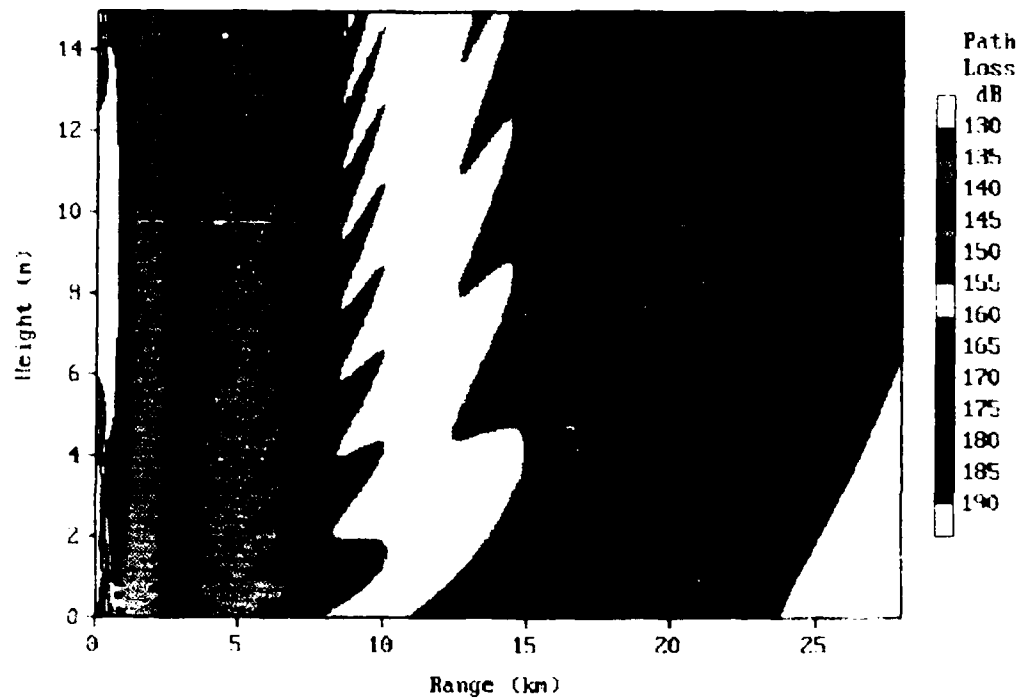fig. 6b   Coverage diagram for the S-band configuration at average sea-level and a duct height of 20 metre.
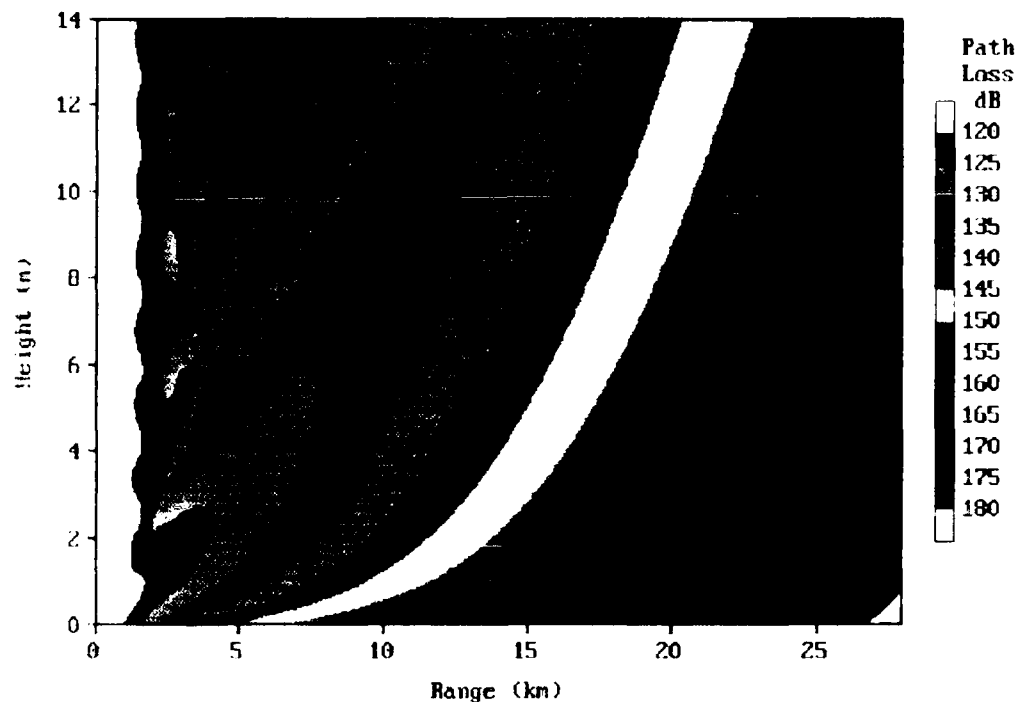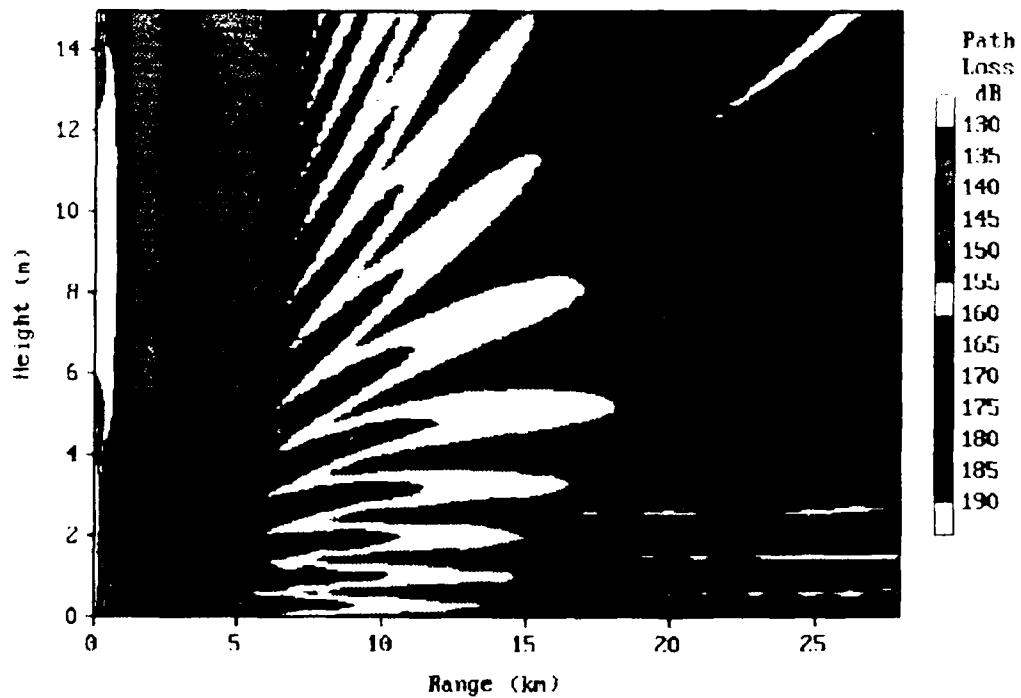
fig. 6c    Coverage diagram for the Ku-band configuration at average sea-level and a duct height of 0 metre.
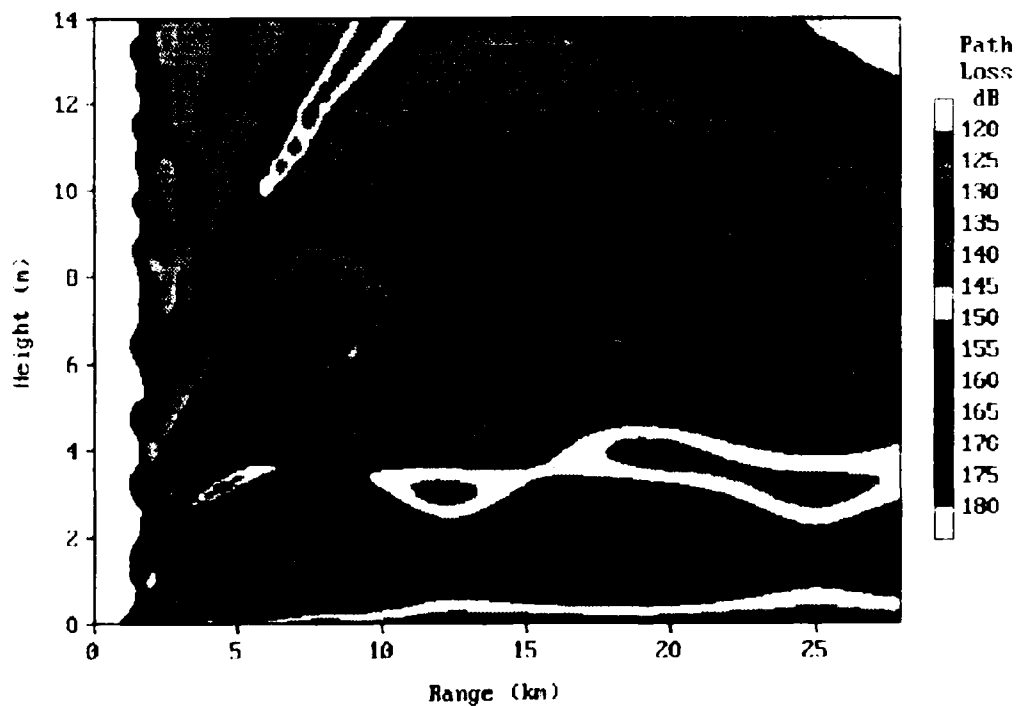


fig. 6d    Coverage diagram for the Ku-band configuration at average sea-level and a duct height of 20 metre.

fig. 6e    Coverage diagram for the W-band configuration at average sea-level and a duct height of
0 metre.



fig. 6f    Coverage diagram for the W-band configuration at average sea-level and a duct height of 10 metre
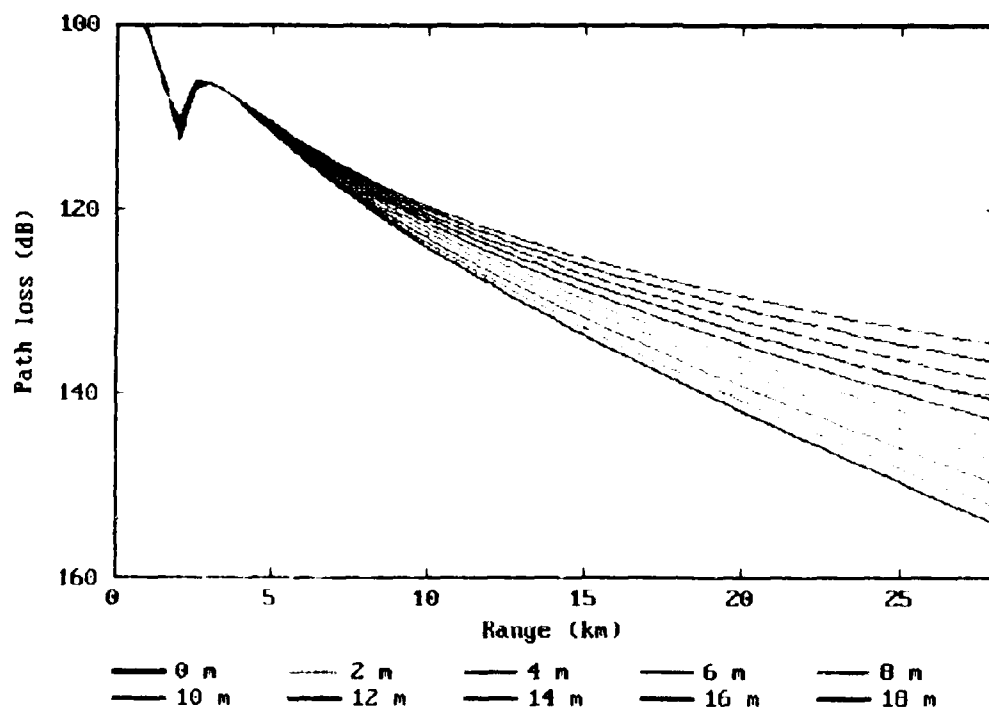
fig. 7a        Range plot for the S-band configuration, at average sea-level and various duct heights.
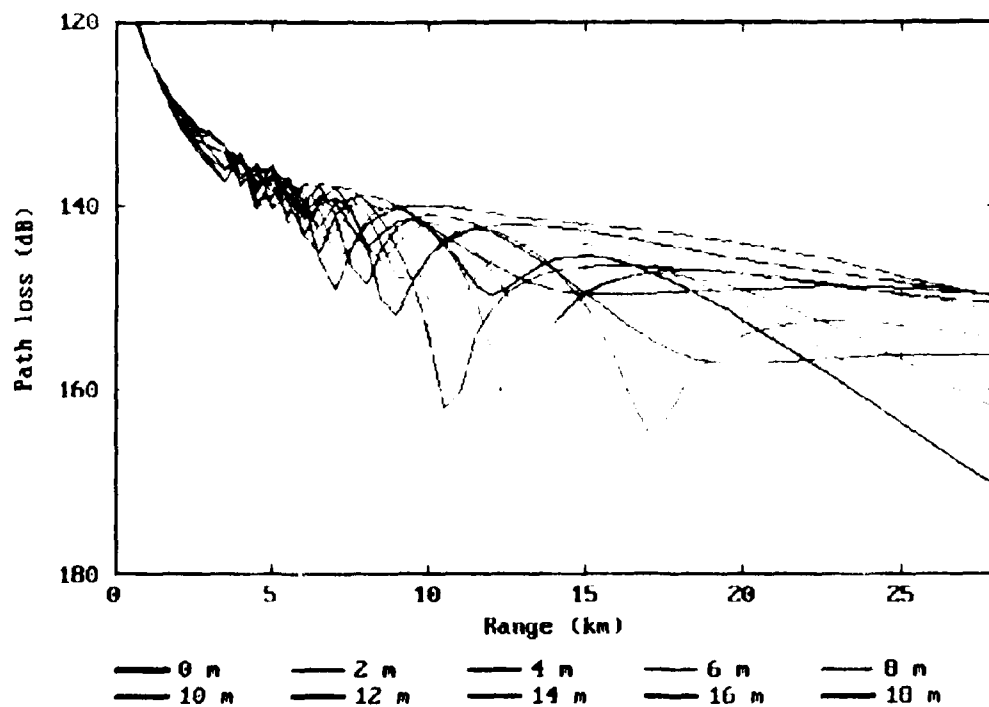


fig. 7b        Range plot for the Ka-band configuration, at average sea-level and various duct heights.

```
                        LORIENT SITUATION
    80                                               FREQ      GHz     3
P                prop.loss=f(SBD) for average sealevel   POLARIZATION    HOR
R                                                    TRAN HT   m    8.37
O                                                    REC HT    m    10.4
P    104                                             ANT TYPE      SINX/X
A                        30 m EVD (max. enhancement)  VER BW    deg     7
G                                                 □   ELEV ANG  deg     0
A
T    128                                          □   EVD HT    m       0
I                                                     SBD HT    m       0
O                        0 m EVD                   □   K             1.333
N                                                    NSUBS           339
     152                                          □   ABS HUM   g/m3  7.5
L                                                    WIND SP   kts    10
O                                                 □
S
S    176    surface based ductheights:           □   FREE-SPACE RANGE
            0,20,30,40,50,60,70,80 m                 or dB THRESHOLDS
d                                                 □              km  27.7
B                                                 □
     200                                          □
        0         8        16       24  27.7  32
                    RANGE  km                        FREE SPACE  - - - -
```
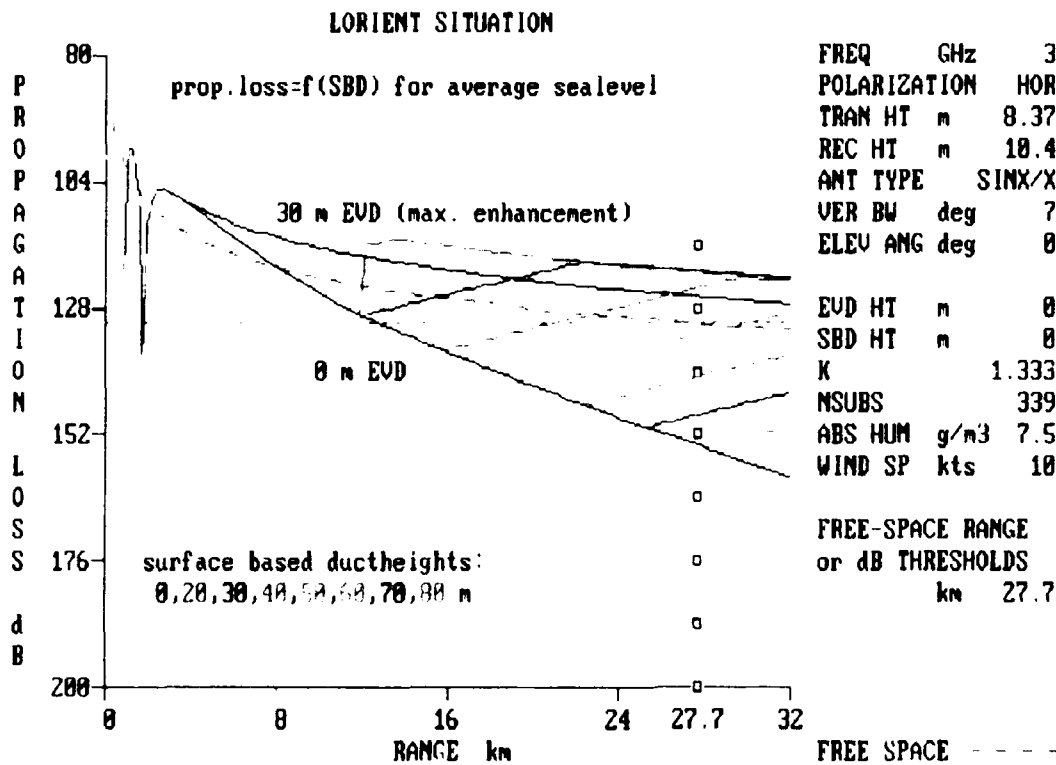
fig. 8    Range plot presenting the influence of surface-based duct for the Lorient S-band configuration.
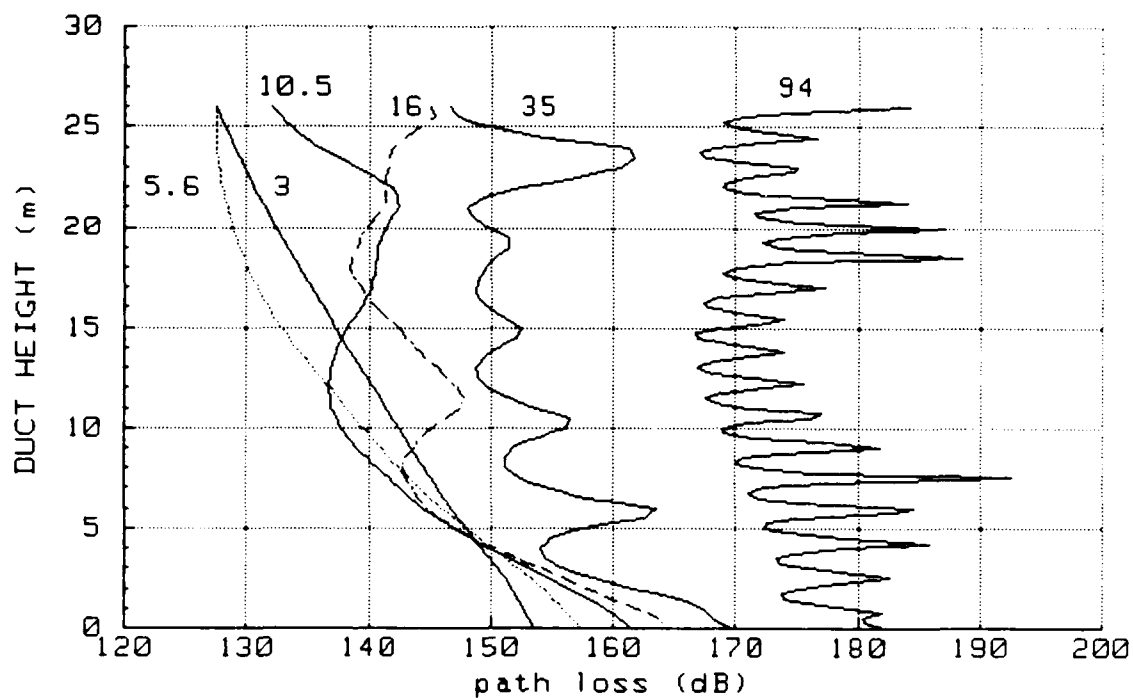
fig. 9a    Influence of the evaporation duct on the path loss for the six propagation sets at average
sea level.
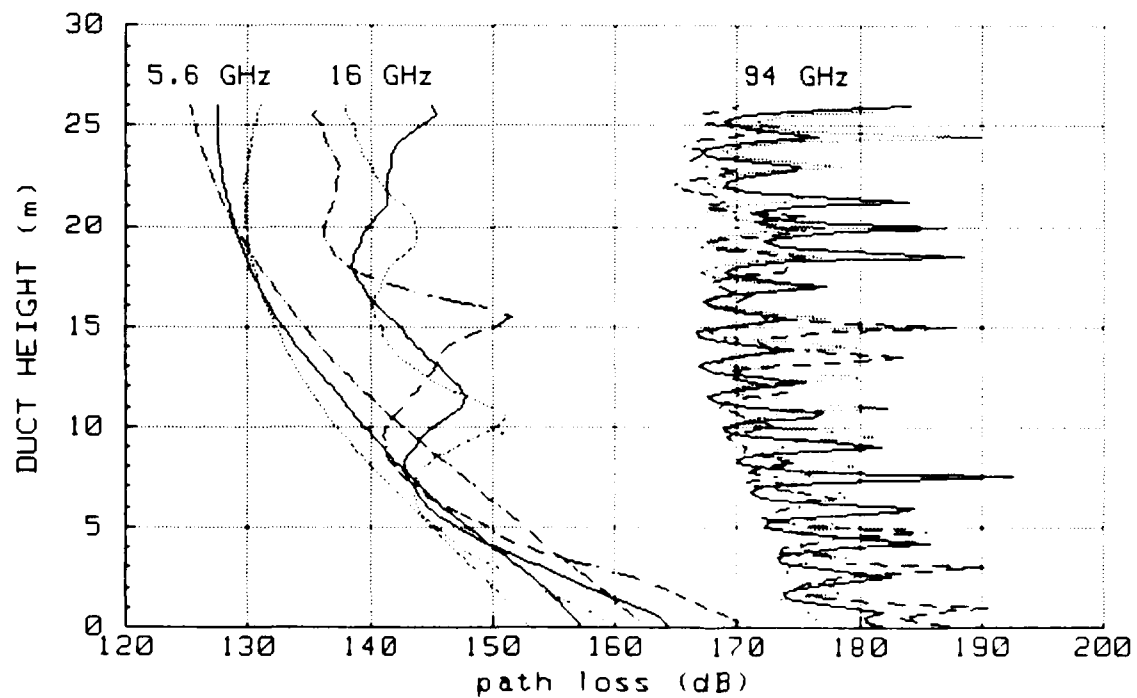


fig. 9b    Infuence of the tide and evaporation duct on the path loss for three propagation sets.
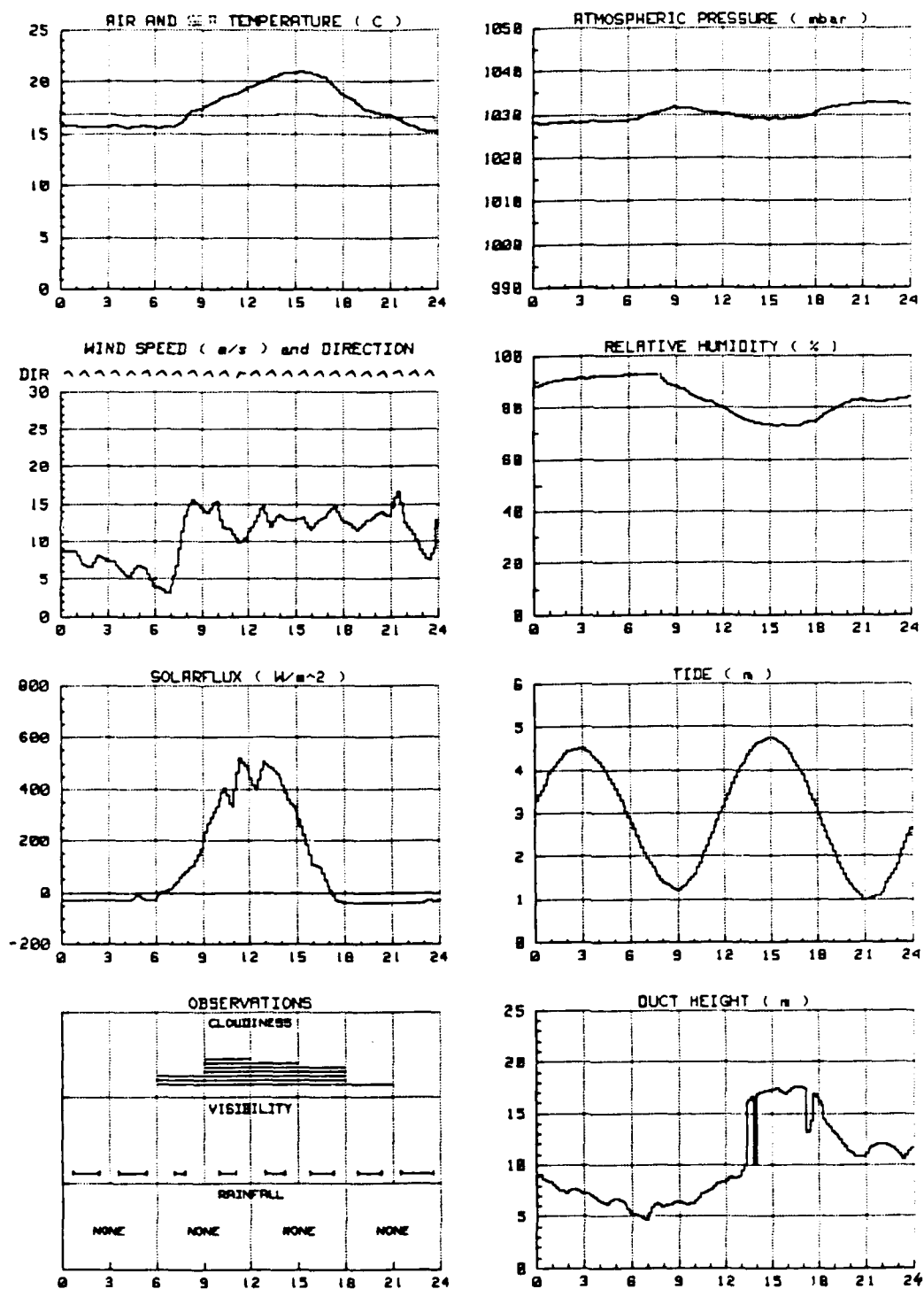
fig. 10a   Meteorological report of 28 September 1989.
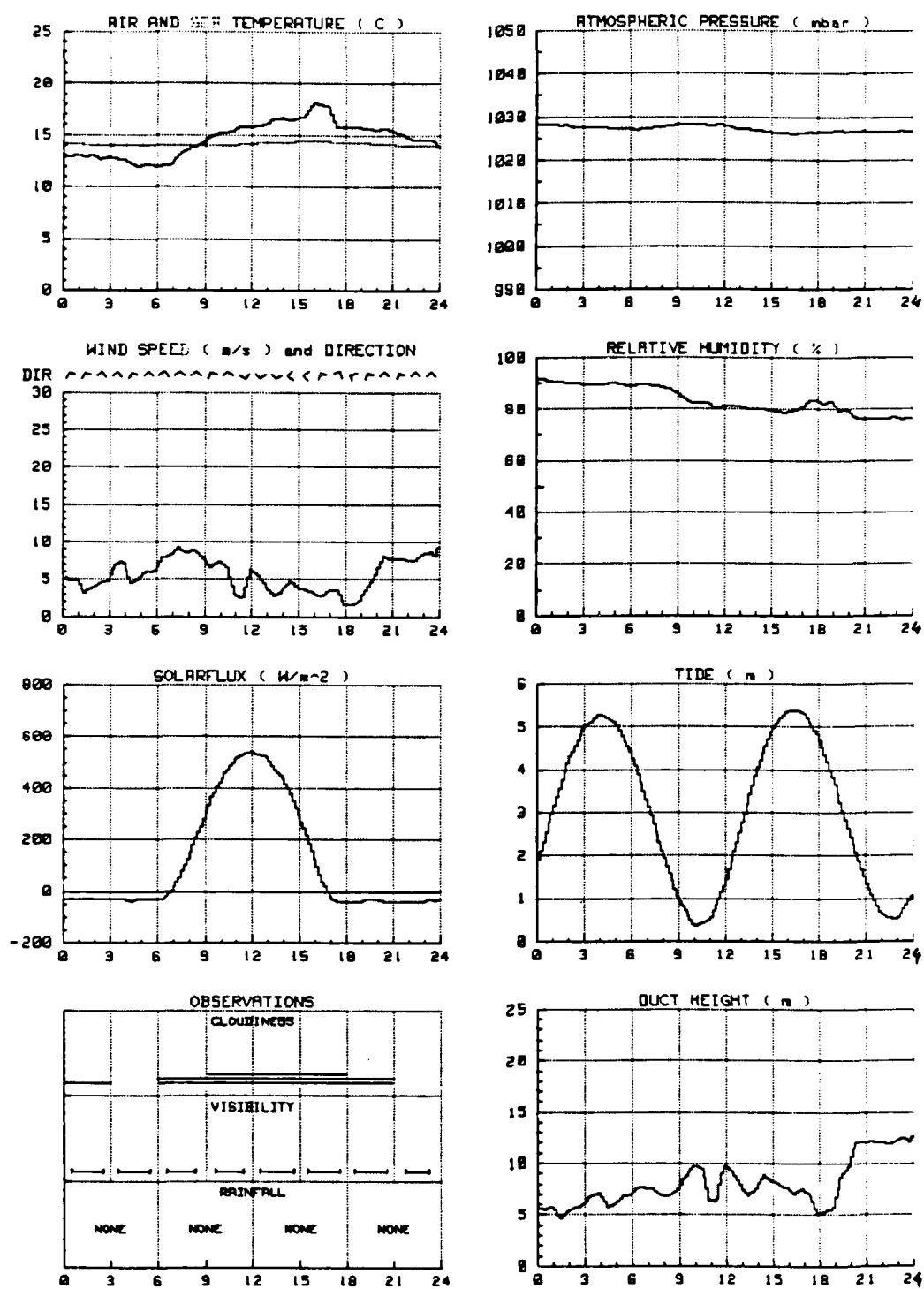
fig. 10b Meteorological report of 16 October 1989.
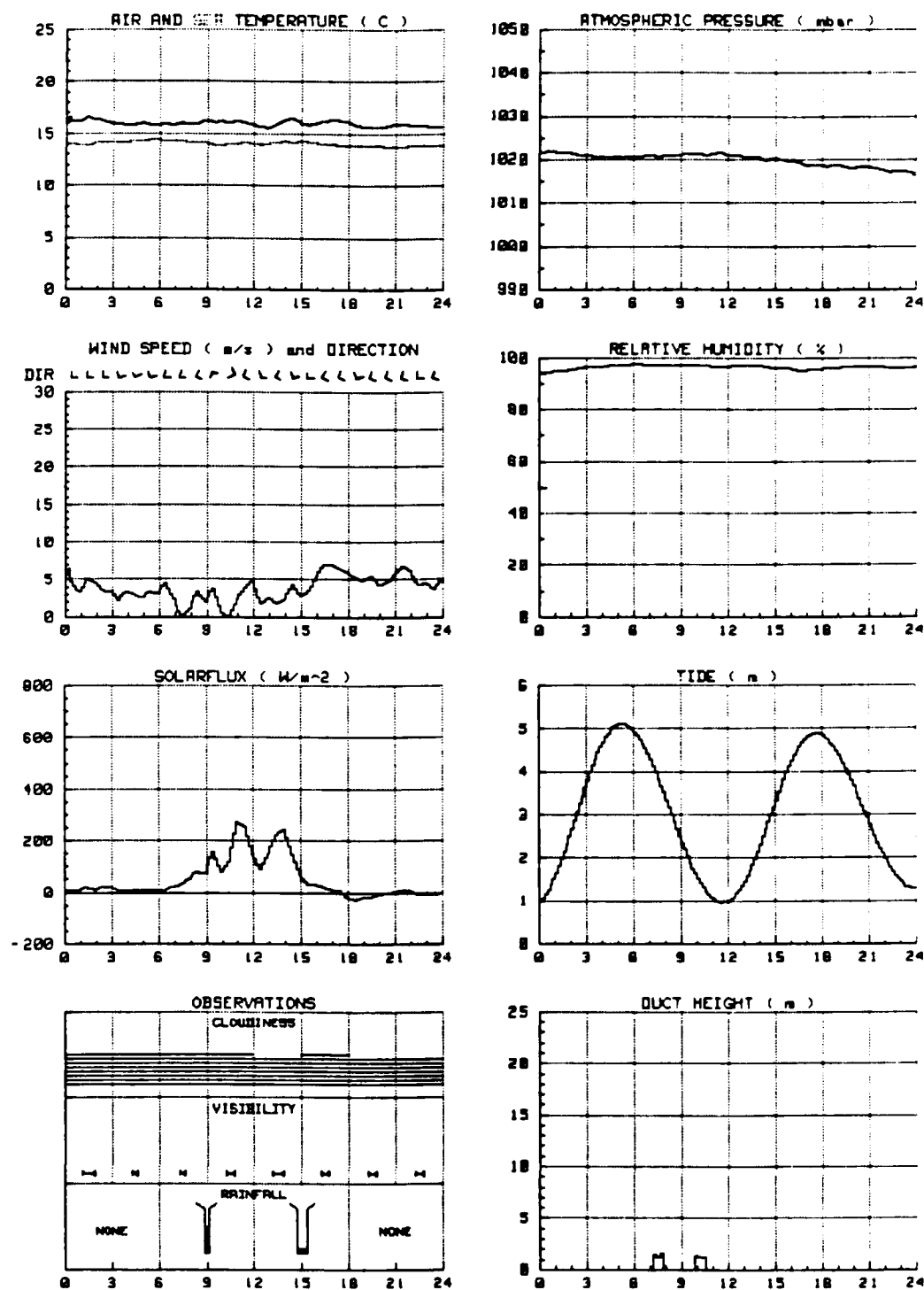
fig. 10c   Meteorological report of 18 October 1989.
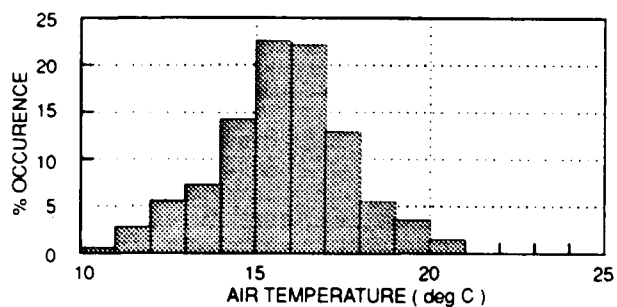
fig. 11a   Air-temperature statistics.
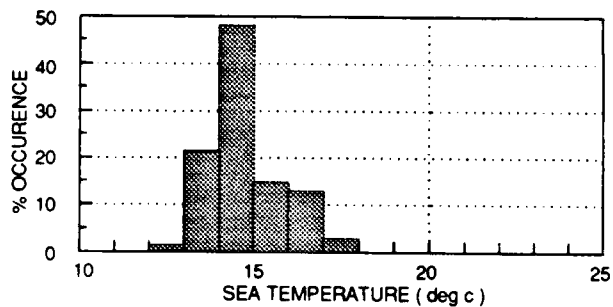
fig. 11b   Sea-temperature statistics.
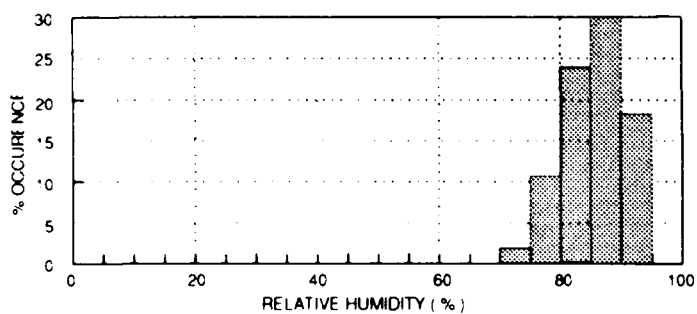
fig. 11c   Relative-humidity statistics.
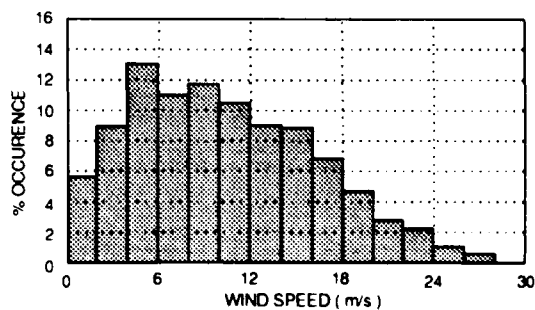
fig. 11d   Wind-speed statistics.

= UNSTABLE SITUATIONS
occurence  27 8%

= UNSTABLE SITUATIONS
occurence  57 4%

= R1b > 0 1 SITUATIONS
occurence  14 8%
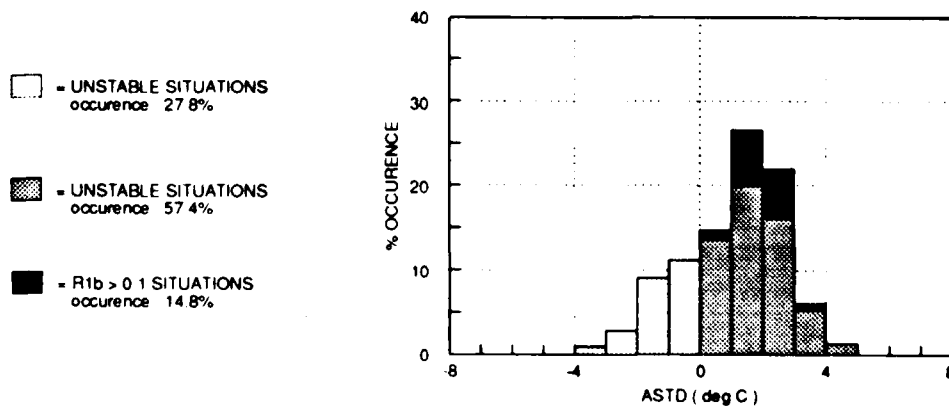
fig. 12   Air-sea temperature difference statistics.

| DUCT HEIGHT | % OCCUR |
|---|---|
| 0 to 1 m | 24.1 |
| 1 to 2 m | 5.1 |
| 2 to 3 m | 6.1 |
| 3 to 4 m | 5.2 |
| 4 to 5 m | 6.5 |
| 5 to 6 m | 5.2 |
| 6 to 7 m | 5.1 |
| 7 to 8 m | 6.7 |
| 8 to 9 m | 5.7 |
| 9 to 10 m | 5.3 |
| 10 to 11 m | 6.8 |
| 11 to 12 m | 6.9 |
| 12 to 13 m | 6.2 |
| 13 to 14 m | 2.4 |
| 14 to 15 m | 0.5 |
| 15 to 16 m | 0.7 |
| 16 to 17 m | 0.4 |
| 17 to 18 m | 0.4 |
| 18 to 19 m | 0.5 |
| 19 to 20 m | 0.1 |
| 20 to 21 m | 0.0 |
| 21 to 22 m | 0.1 |
| 22 to 23 m | 0.0 |
| 23 to 24 m | 0.0 |
| 24 to 25 m | 0.0 |
| 25 to 26 m | 0.0 |
| 26 to 27 m | 0.0 |
| 27 to 28 m | 0.0 |



fig. 13    Statistics of the duct heights calculated with the Paulus formulation.

| DUCT HEIGHT | % OCCUR |
|---|---|
| 0 to 1 m | 17.3 |
| 1 to 2 m | 6.0 |
| 2 to 3 m | 7.2 |
| 3 to 4 m | 7.6 |
| 4 to 5 m | 10.8 |
| 5 to 6 m | 13.8 |
| 6 to 7 m | 9.2 |
| 7 to 8 m | 8.9 |
| 8 to 9 m | 4.6 |
| 9 to 10 m | 2.1 |
| 10 to 11 m | 1.1 |
| 11 to 12 m | 1.0 |
| 12 to 13 m | 1.2 |
| 13 to 14 m | 1.1 |
| 14 to 15 m | 0.8 |
| 15 to 16 m | 0.7 |
| 16 to 17 m | 1.3 |
| 17 to 18 m | 0.9 |
| 18 to 19 m | 0.9 |
| 19 to 20 m | 0.9 |
| 20 to 21 m | 0.6 |
| 21 to 22 m | 0.4 |
| 22 to 23 m | 0.4 |
| 23 to 24 m | 0.3 |
| 24 to 25 m | 0.4 |
| 25 to 26 m | 0.2 |
| 26 to 27 m | 0.2 |
| 27 to 28 m | 0.0 |



fig. 14    Statistics of the optimum duct heights derived from the measured path losses.

## RECEIVED SIGNALS LORIENT CAMPAIGN

3 GHz    5 h   GH₂                    16 GHz   35 GHz  94 GHz
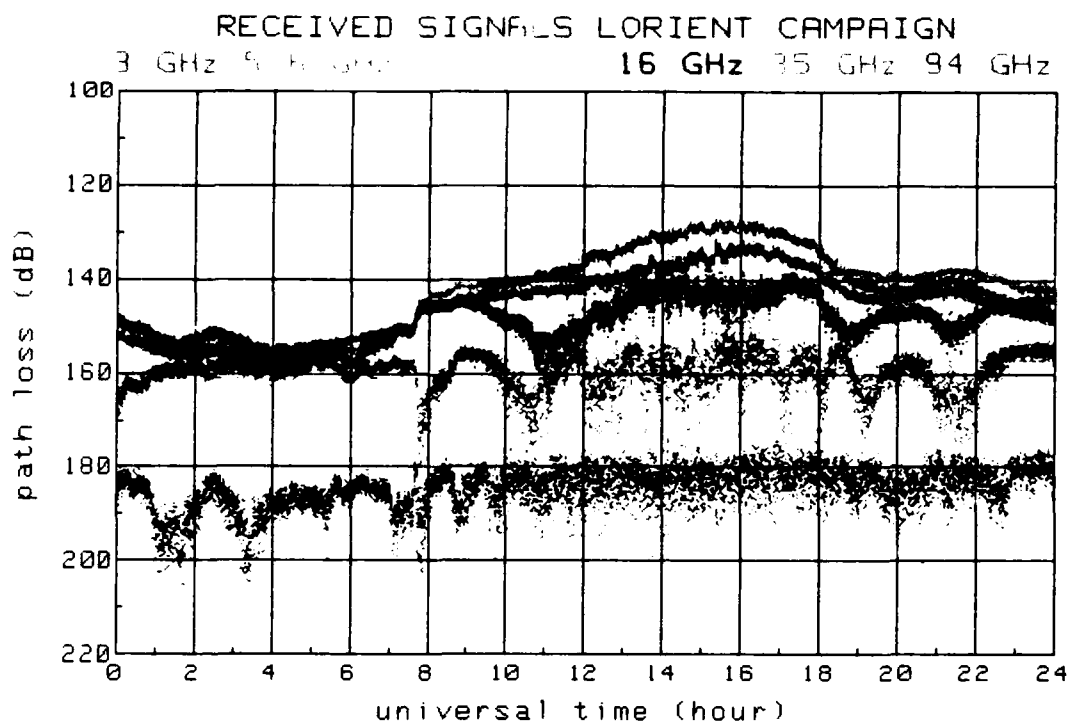
fig. 15a   Measured path losses of 28 September 1989.

## RECEIVED SIGNALS LORIENT CAMPAIGN

3 GHz    5 h   GH₂                    16 GHz   35 GHz  94 GHz
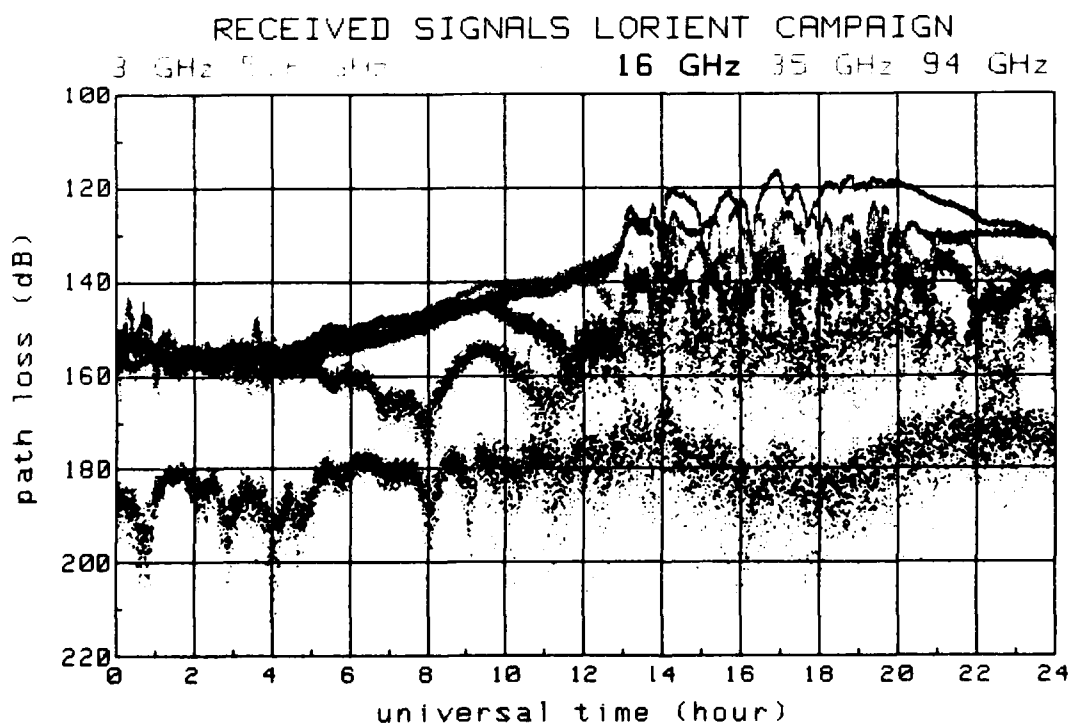
fig. 15b   Measured path losses of 16 October 1989.

RECEIVED SIGNALS LORIENT CAMPAIGN

3 GHz 5 6 GHz          16 GHz  35 GHz  94 GHz
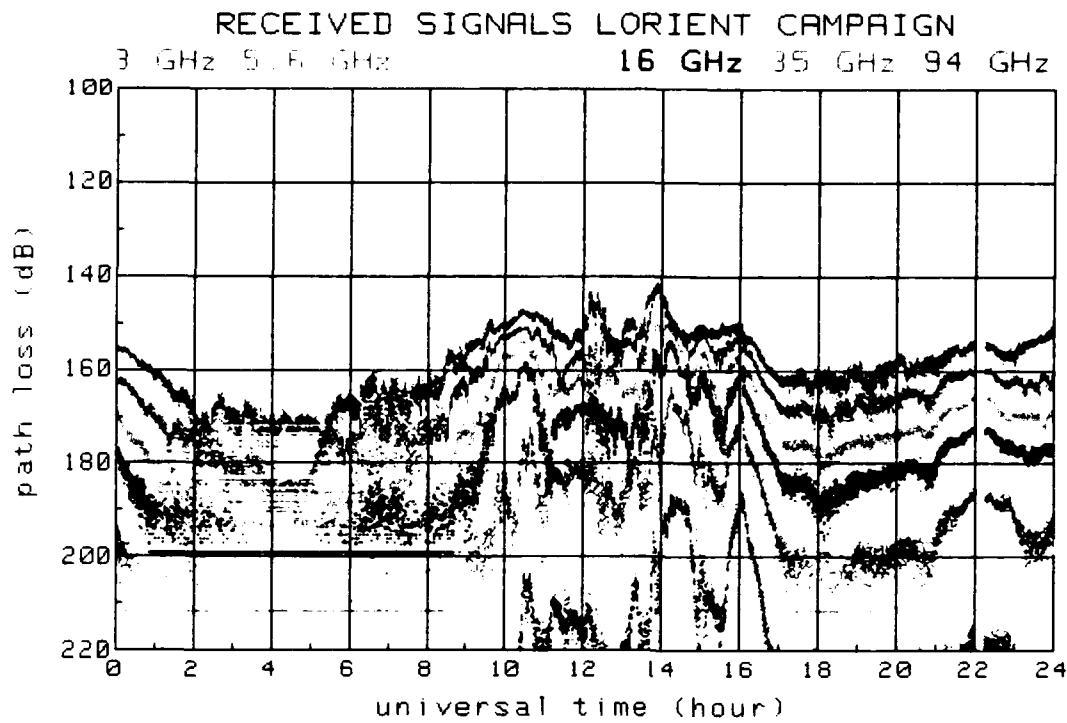
fig. 15c  Measured path losses of 18 October 1989.

MEASURED and PREDICTED PATH LOSS

3 GHz 5 6 GHz          16 GHz  35 GHz  94 GHz
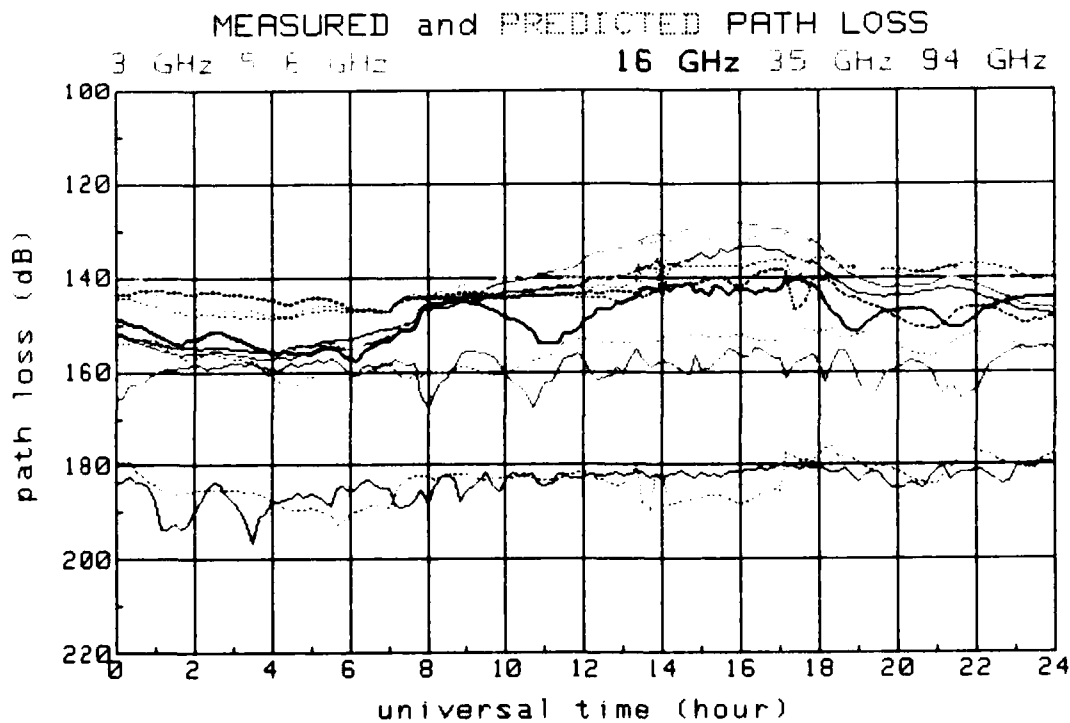
fig. 16    Path loss comparison for 28 September 1989.
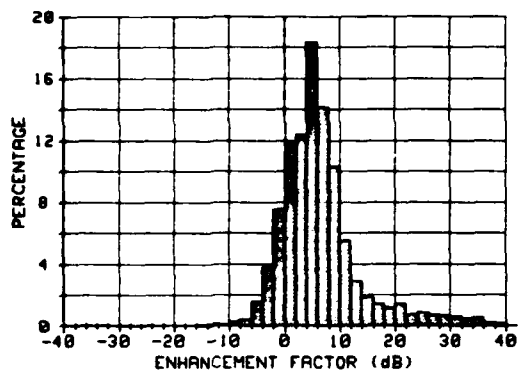
fig. 17a   3 GHz statistics
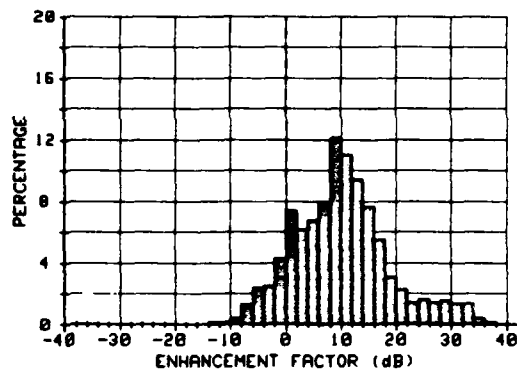
fig. 17b   5.6 GHz statistics
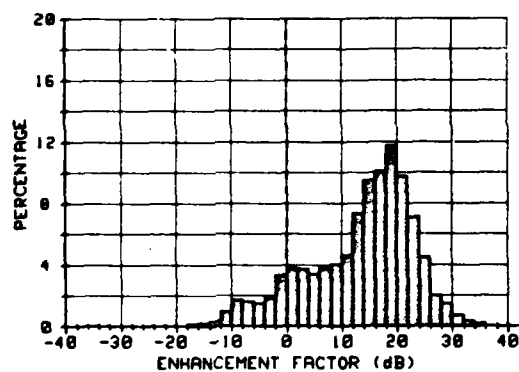
fig. 17c   10.5 GHz statistics
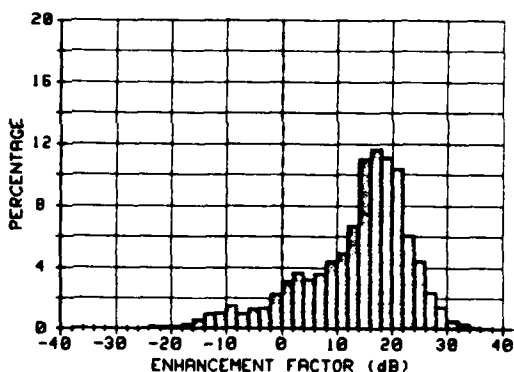
fig. 17d   16 GHz statistics
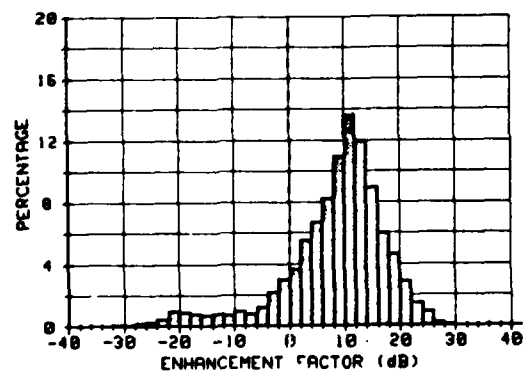
fig. 17e   35 GHz statistics
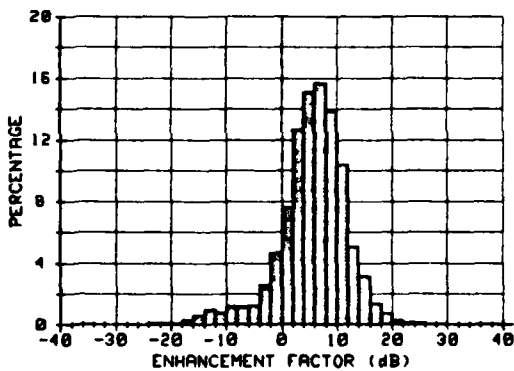
fig. 17f   94 GHz statistics

fig. 17   Enhancement factor statistics of measured data.

SCATTERPLOT COMPARISON (predicted to measured path loss)

FREQUENCY: 3 GHz

MEASUREMENT PERIOD:
23 Sept 1989 - 13 Nov 1989

TOTAL NUMBER OF POINTS: 7278

DISTINGUISHED DATA:
stable atmosphere situation
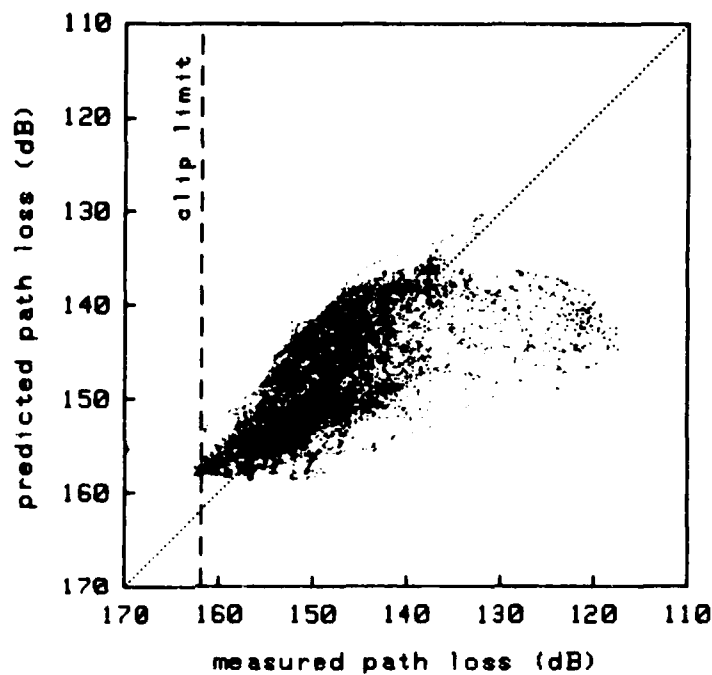
DEVIATION (predicted-measured path loss)

| = average deviation

| = rms deviation

Total rms deviation: 5.3 dB
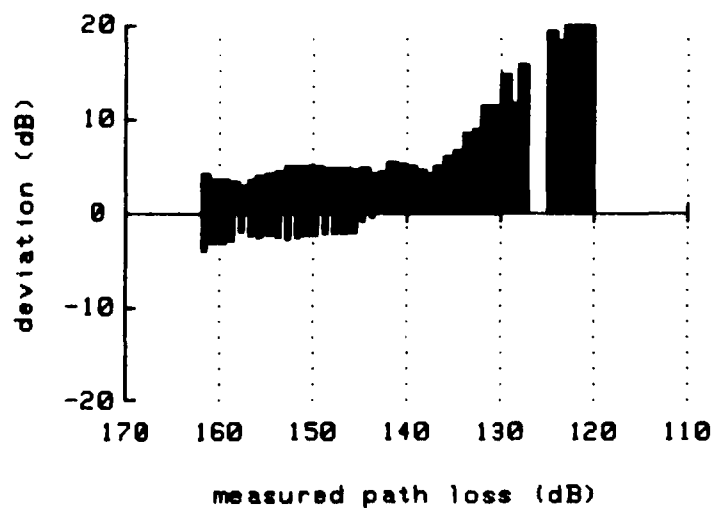
fig. 18a   Comparison between the measured and predicted 3 GHz path losses of the Lorient period.
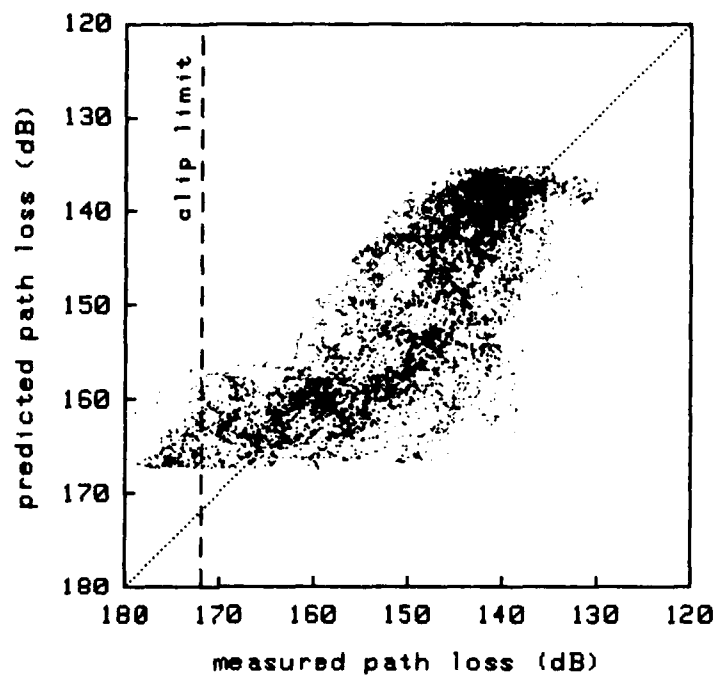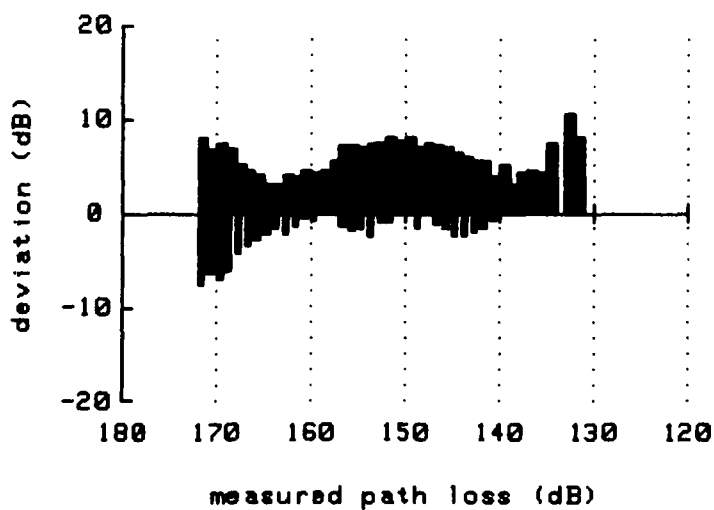
SCATTERPLOT COMPARISON (predicted to measured path loss)

FREQUENCY: 5.6 GHz

MEASUREMENT PERIOD:
23 Sept 1989 — 13 Nov 1989

TOTAL NUMBER OF POINTS: 7239

DISTINGUISHED DATA:
bulk Richardson number   .1
stable atmosphere situation
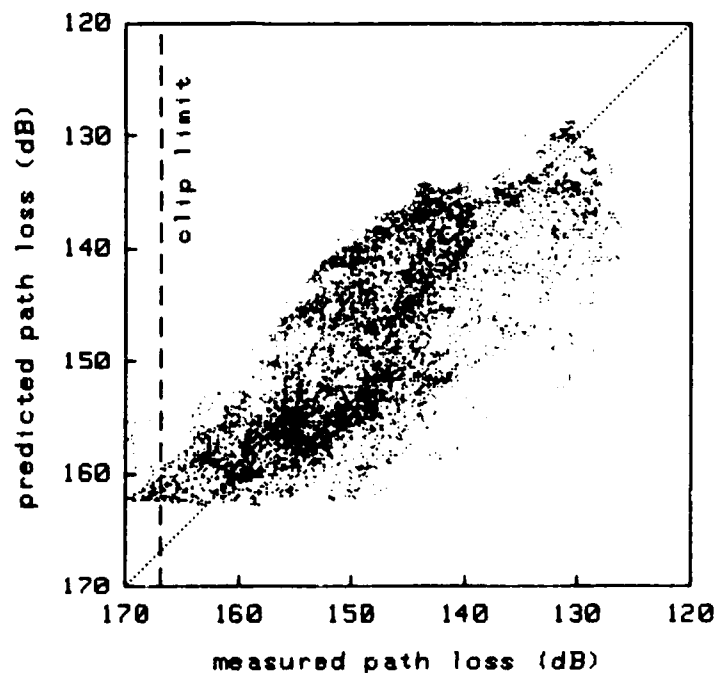


DEVIATION (predicted-measured path loss)

▌ = average deviation

▐ = rms deviation

Total rms deviation: 6.2 dB
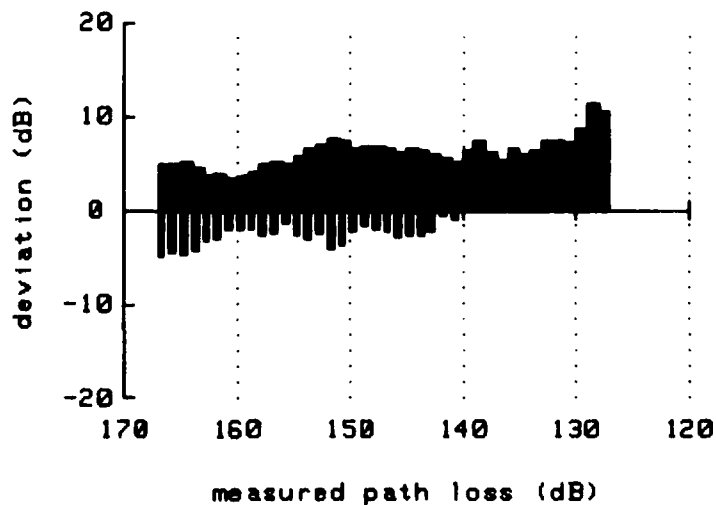


fig. 18b  Comparison between the measured and predicted 5.6 GHz path losses of the Lorient period.
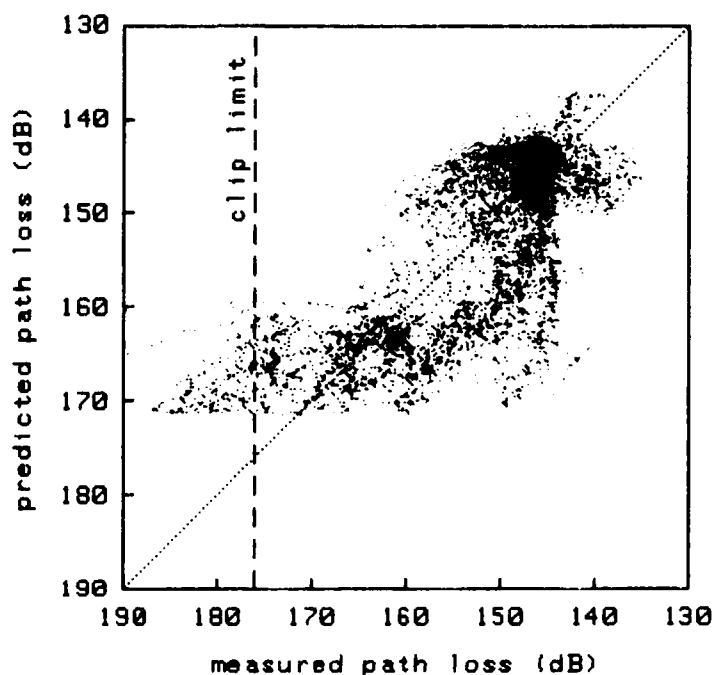
SCATTERPLOT COMPARISON (predicted to measured path loss)

FREQUENCY: 10.5 GHz

MEASUREMENT PERIOD:
23 Sept 1989 - 13 Nov 1989

TOTAL NUMBER OF POINTS: 7246

DISTINGUISHED DATA:
b. l. Richardson number ... l
stable atmosphere situation
... ... ... ... ... ... ... ...

DEVIATION (predicted-measured path loss)

| = average deviation

▮ = rms deviation

Total rms deviation: 6.1 dB

fig. 18c  Comparison between the measured and predicted 10.5 GHz path losses of the Lorient period.
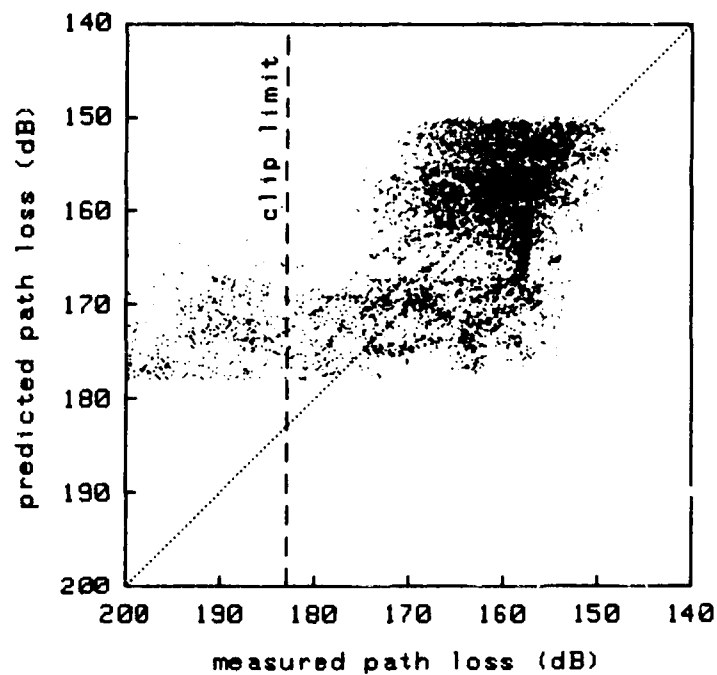
SCATTERPLOT COMPARISON (predicted to measured path loss)

FREQUENCY: 16 GHz

MEASUREMENT PERIOD:
23 Sept 1989 - 13 Nov 1989

TOTAL NUMBER OF POINTS: 7249

DISTINGUISHED DATA:
☐ = measurement number ...
stable atmosphere situation
... = ...

DEVIATION (predicted-measured path loss)

▌ = average deviation
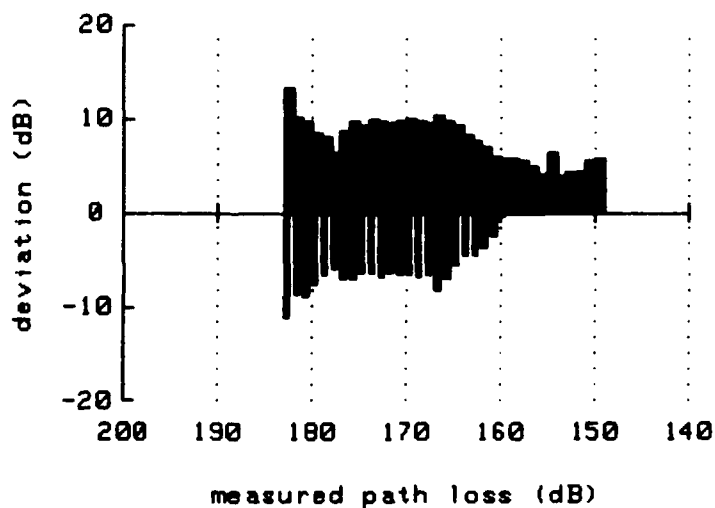
▌ = rms deviation

Total rms deviation: 6.5 dB

fig. 18d   Comparison between the measured and predicted 16 GHz path losses of the Lorient period.

SCATTERPLOT COMPARISON (predicted to measured path loss)

FREQUENCY: 35 GHz

MEASUREMENT PERIOD:
23 Sept 1989 - 13 Nov 1989

TOTAL NUMBER OF POINTS: 7149

DISTINGUISHED DATA:
bulk Richardson number: ... 1
stable atmosphere situation

DEVIATION (predicted-measured path loss)

▌ = average deviation

▌ = rms deviation

Total rms deviation: 7.6 dB

fig. 18e   Comparison between the measured and predicted 35 GHz path losses of the Lorient period.

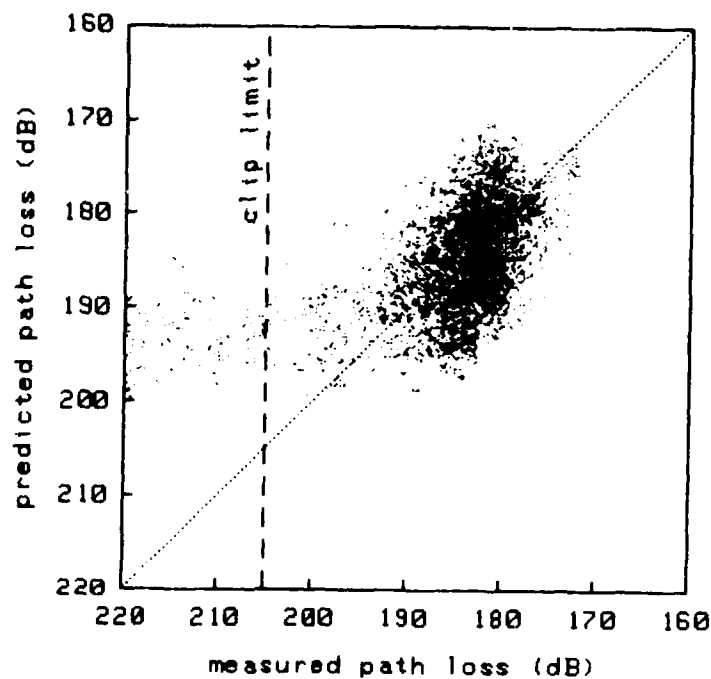SCATTERPLOT COMPARISON (predicted to measured path loss)

FREQUENCY: 94 GHz

MEASUREMENT PERIOD:
23 Sept 1989 - 13 Nov 1989

TOTAL NUMBER OF POINTS: 5843

DISTINGUISHED DATA:
stable atmosphere situation

DEVIATION (predicted-measured path loss)

| = average deviation
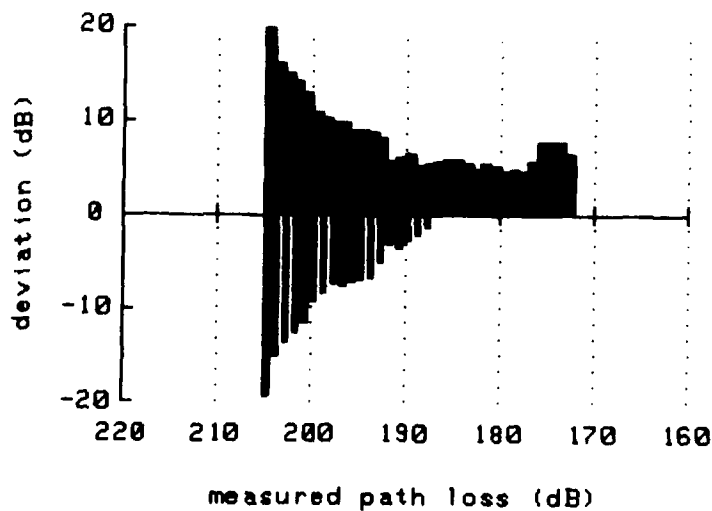
▮ = rms deviation

Total rms deviation: 6.1 dB

fig. 18f   Comparison between the measured and predicted 94 GHz path losses of the Lorient period.

Duct heights 28 September 1989
calculated from measured signals for:
8 GHz             16 GHz
calculated from meteo data: UNSTABLE
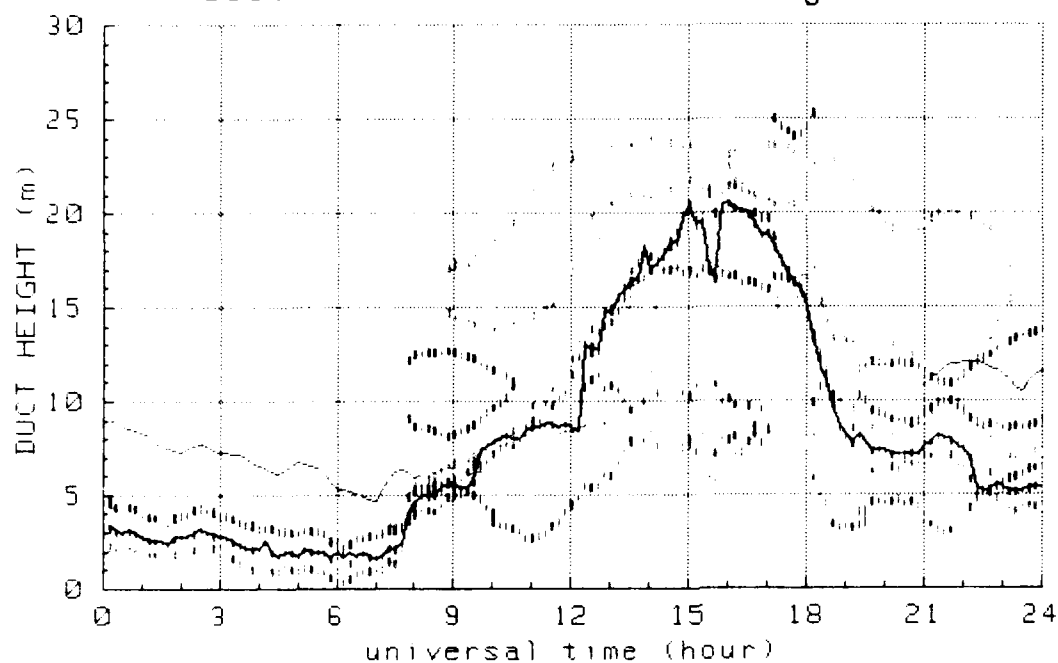Best fit for all measured signals

fig. 19    Presentation of the duct height predicted from the meteo data and the determination of the
optimum duct height.

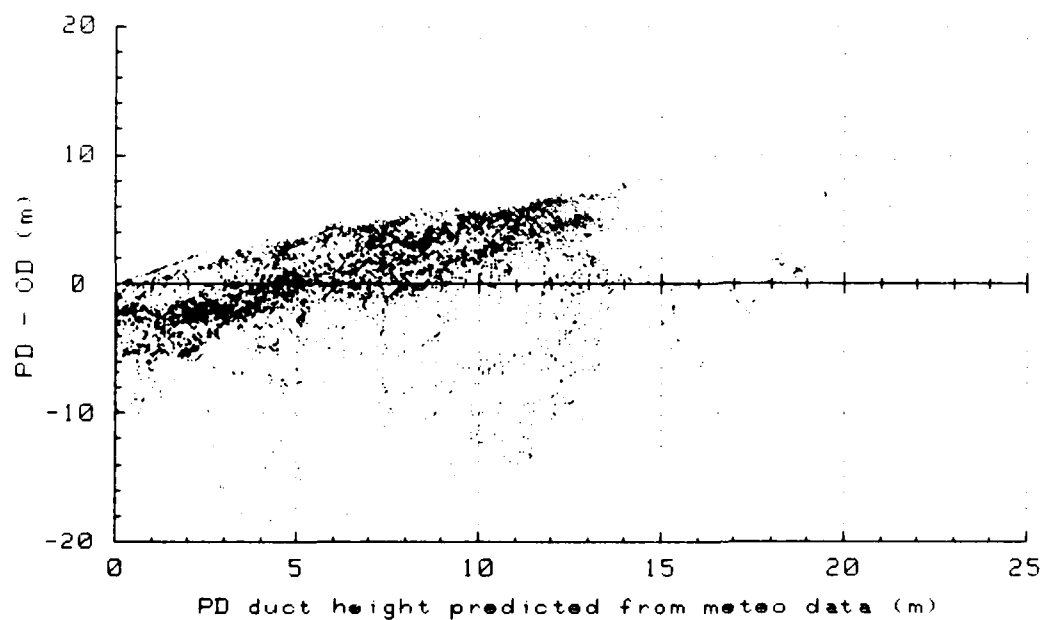ATMOSPHERICAL SITUATION:          , STABLE,

fig. 20    Comparison of optium duct heights derived from measured path losses (OD) with duct heights
predicted from meteo data (PD).
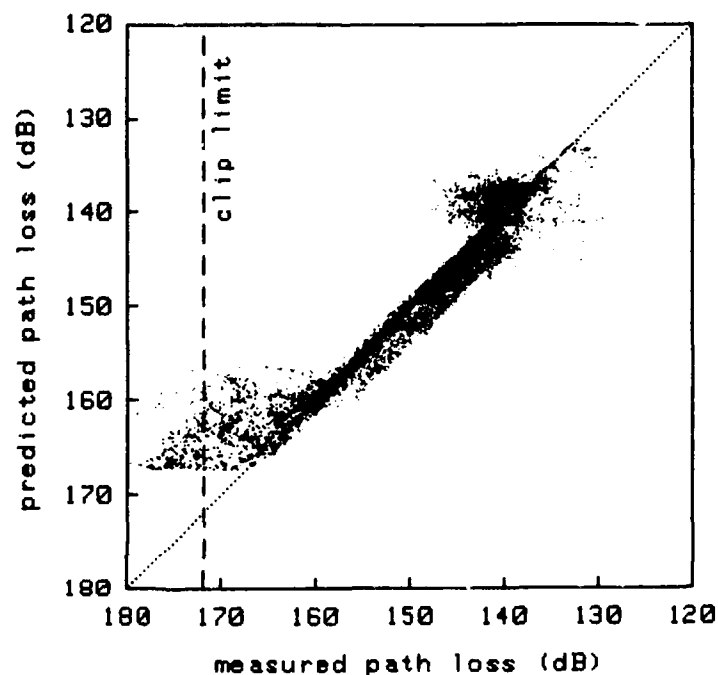
SCATTERPLOT COMPARISON (predicted to measured path loss)

FREQUENCY: 10.5 GHz

MEASUREMENT PERIOD:
23 Sept 1989 - 13 Nov 1989

TOTAL NUMBER OF POINTS: 7398

DISTINGUISHED DATA:
bulk Richardson number
stable atmosphere situation

DEVIATION (predicted-measured path loss)

| = average deviation
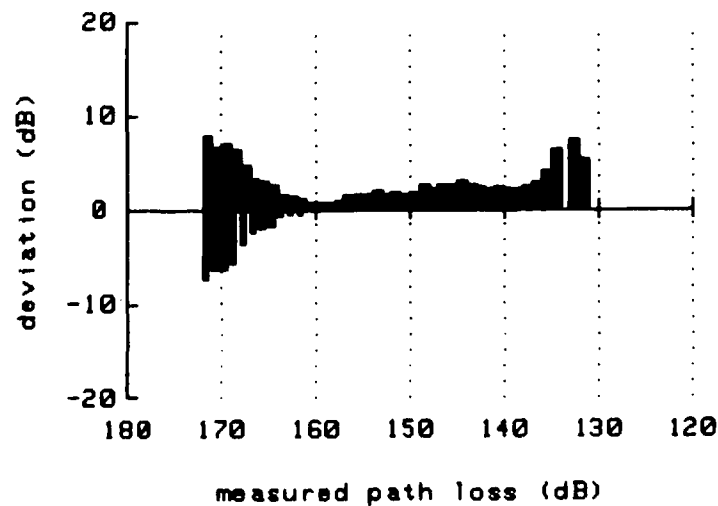
▌ = rms deviation

Total rms deviation: 2.6 dB

fig. 21    Comparison between measured 10.5 GHz pathlosses and the path losses predicted from the
optimum duct heights.

# REPORT DOCUMENTATION PAGE          (MOD-NL)

| 1. DEFENSE REPORT NUMBER (MOD-NL) | 2. RECIPIENT'S ACCESSION NUMBER | 3. PERFORMING ORGANIZATION REPORT NUMBER |
|---|---|---|
| TD93-0303 | | FEL-92-B438 |

| 4. PROJECT/TASK/WORK UNIT NO. | 5. CONTRACT NUMBER | 6. REPORT DATE |
|---|---|---|
| 6134.20 | | JULY 1993 |

| 7. NUMBER OF PAGES | 8. NUMBER OF REFERENCES | 9. TYPE OF REPORT AND DATES COVERED |
|---|---|---|
| 68 ( INCL. EXECUTIVE SUMMARY AND 1 APPENDIX, EXCL. RDP & DISTRIBUTION LIST) | 5 | |

**10. TITLE AND SUBTITLE**
OVER-THE-HORIZON PROPAGATION MEASUREMENT AT SIX RADAR-FREQUENCY BANDS AT THE ATLANTIC OCEAN COAST.

**11. AUTHOR(S)**
R.B. BOEKEMA

**12. PERFORMING ORGANIZATION NAME(S) AND ADDRESS(ES)**
TNO PHYSICS AND ELECTRONICS LABORATORY, P.O. BOX 96864, 2509 JG THE HAGUE
OUDE WAALSDORPERWEG 63, THE HAGUE, THE NETHERLANDS

**13. SPONSORING/MONITORING AGENCY NAME(S)**
TNO PHYSICS AND ELECTRONICS LABORATORY, P.O. BOX 96864, 2509 JG THE HAGUE
OUDE WAALSDORPERWEG 63, THE HAGUE, THE NETHERLANDS

**14. SUPPLEMENTARY NOTES**
EXPERIMENTAL DATA IS GATHERED IN A NATO AC/243 (PANEL3/RSG8) CO-OPERATION.
THE CLASSIFICATION DESIGNATION ONGERUBRICEERD IS EQUIVALENT TO UNCLASSIFIED.

**15. ABSTRACT (MAXIMUM 200 WORDS, 1044 POSITIONS)**

IN THE AUTUMN OF 1989 THE PROPAGATION SUBGROUP OF NATO AC/243 (PANEL3/RSG8) HAS CONDUCTED A PROPAGATION EXPERIMENT NEAR BREST FRANCE, AT THE ATLANTIC OCEAN. PURPOSE OF THIS EXPERIMENT WAS TO GAIN AN INSIGHT INTO THE INFLUENCE OF EVAPORATION DUCT ABOVE THE SEA ON THE PROPAGATION OF RADAR SIGNALS WITH DIFFERENT FREQUENCIES FOR AN OVER-THE-HORIZON SITUATION, AND INTO THE APPLICABILITY OF MODEL PREDICTIONS. PARTICIPATING NATIONS WERE THE UNITED STATES, FRANCE, GERMANY AND THE NETHERLANDS. AS DUTCH REPRESENTATIVE, THE TNO PHYSICS AND ELECTRONICS LABORATORY HAS MEASURED PATH LOSSES CONTINUOUSLY DURING A PERIOD OF 52 DAYS AT 3, 5.6, 10.5, 16, 35 AND 94 GHZ FOR A 27.7 KM OVER-THE-HORIZON PATH. THE GEOMETRY OF THE EXPERIMENT HAS BEEN CHOSEN TO REPRESENT A TYPICAL SHIP DEFENCE SITUATION. THE MEASUREMENTS HAVE SHOWN THAT FOR THE PRESENT CASE THE NEARLY ALWAYS PRESENT EVAPORATION DUCT RESULTS IN A SIGNAL ENHANCEMENT WITH THE STRONGEST EFFECTS AT THE 10.5 AND 16 GHZ FREQUENCIES. AN EXTENDED STUDY OF THE QUALITY OF THE MODEL PREDICTIONS, POSSIBLE BY THE UNIQUE SET OF MEASUREMENT RESULTS, SHOWS SOME INTERESTING MATTERS. IF WE DIVIDE THE PROCESS OF PREDICTION INTO TWO PARTS, THE CALCULATION OF THE DUCT HEIGHT FROM THE METEOROLOGICAL DATA AND THE PATH LOSS CALCULATION FROM THIS DUCT HEIGHT, WE COME TO THE CONCLUSION THAT THE FIRST PART IS RESPONSIBLE FOR THE LARGEST INACCURACIES. THE USED DUCT HEIGHT CALCULATION METHOD SHOWED SYSTEMATIC DEVIATIONS FOR DIFFERENT METEOROLOGICAL CONDITIONS. THE INACCURACY OF THE DUCT HEIGHT CALCULATION MAKES USEFUL PATH LOSS PREDICTIONS AT THE MILLIMETRE-WAVE FREQUENCIES (35 AND 94 GHZ) IMPOSSIBLE FOR THIS OVER-THE-HORIZON SITUATION. THE PREDICTIONS AT THE LOWER FREQUENCIES ARE MUCH BETTER, BUT NOT ALWAYS SATISFACTORY. THE DEVIATION ANALYSES IN THIS REPORT CAN BE USEFUL TO IMPROVE PROPAGATION MODELS.

| 16. DESCRIPTORS | IDENTIFIERS |
|---|---|
| PROPAGATION OF RADAR WAVES NORTH ATLANTIC OCEAN | OVER-THE-HORIZON PROPAGATION PROPAGATION MEASUREMENT |

| 17a. SECURITY CLASSIFICATION (OF REPORT) | 17b. SECURITY CLASSIFICATION (OF PAGE) | 17c. SECURITY CLASSIFICATION (OF ABSTRACT) |
|---|---|---|
| ONGERUBRICEERD | ONGERUBRICEERD | ONGERUBRICEERD |

| 18. DISTRIBUTION/AVAILABILITY STATEMENT | 17d. SECURITY CLASSIFICATION (OF TITLES) |
|---|---|
| UNLIMITED | ONGERUBRICEERD |